AN ABSTRACT OF THE THESIS OF

Ronald J. Fehringer for the degree of Master of Science in Bioresource Engineering presented on September 10, 1990.

Title: A Comparison of Drift from Hooded and Open-Boom Agricultural Sprayers

Abstract approved: Redacted for Privacy

Professor Richard A. Cavaletto

A recent development in drift-control for agricultural ground sprayers is the installation of a hood (or shroud) over the boom. Hoods are designed to provide a protected zone in which droplets can be sprayed and deposited on the target with limited interference from the wind.

This study compared chemical drift using hooded and open-boom pesticide sprayers in various configurations. The hooded sprayer included an air-foil mounted on top of the hood, designed to re-direct the airflow and further decrease drift. The principal objective was to test the performance of the hood, the air-foil, and nozzle size in reducing drift. A fluorescent dye and water solution was sprayed adjacent to a series of parallel string collectors. The amount of drifting material was determined by rinsing the string and testing the fluorescence of the rinsewater. Wind speed and direction, temperature, and relative humidity were monitored during each field test so that the influence of weather conditions on drift could be assessed.

Statistical and graphical comparisons were based on the development of a regression model to describe downwind drift for each sprayer configuration under a set of variable weather conditions. Only parameters found to be important to drift were included in the final model. These parameters included sprayer configuration, wind speed, temperature, and the interactions of configuration with wind speed and temperature.

Results of the comparisons indicated that for a larger droplet spectrum, the hood reduced drift significantly, while for smaller droplets the hood was ineffective. The air-foil was found to have no influence on drift.

A Comparison of Drift from Hooded and Open-Boom Agricultural Sprayers

by

Ronald J. Fehringer

A THESIS

submitted to

Oregon State University

in partial fulfillment of
the requirements for the
degree of

Master of Science

Completed September 10, 1990

Commencement June 1991

APPROVED:

Redacted for Privacy

Professor of Bioresource Engineering in Charge of Major

Redacted for Privacy

Head of the Department of Bioresource Engineering

Redacted for Privacy

Dean of the Graduate School

Date thesis presented September 10, 1990

Thesis written and presented by Ronald J. Fehringer

ACKNOWLEDGEMENTS

I would like to thank those individuals who have made this accomplishment possible. First, thanks to Dr. Richard Cavaletto for bringing me aboard on this project, and for being a friend as well as a mentor. Thanks to Bob Schnekenburger for his help in the tremendous task of assembling and moving the sprayers. I am eternally grateful to my parents, Jerry and Virginia, for their unwaivering support and belief in my abilities. And finally, sincerest thanks to my fiancée, Valerie Sullivan, whose love and encouragement carried me through.

TABLE OF CONTENTS

LIST OF FIGURES

LIST OF TABLES

A COMPARISON OF DRIFT FROM HOODED AND OPEN-BOOM AGRICULTURAL SPRAYERS

1. INTRODUCTION

The drift of agricultural chemicals is a problem from the perspectives of cost and environmental pollution. Higher costs are incurred due to increased chemical requirements, production losses associated with pest competition, and damage to non-target crops. Surface and/or groundwater may be contaminated. Humans, livestock, or food supplies may be accidently exposed to toxic liquids or vapors. Several techniques have been employed to minimize the drift problem, for both aerial and ground-level applications. Operational techniques involve careful timing of the application with weather conditions. Spraying is postponed when a significant wind is blowing toward sensitive areas. Mechanical techniques involve using different or modified equipment and chemicals. Different nozzles or pressures may be used, or for ground rigs the structure of the sprayer may be altered in an attempt to contain the spray droplets. Sometimes alternate chemicals can be selected. Although operational techniques are less expensive and less complicated, they are not always feasible. Waiting for minimal winds may mean missing the critical time window.

For ground rigs, recent emphasis has been placed on structural alterations. Several manufacturer's build sprayers with hoods (or shrouds), shields, air-foils, and air curtains (or skirts), claiming that drift is significantly reduced or eliminated. The effectiveness of such alterations is uncertain due to a lack of actual field data. The goal of this research project was to determine the value of a particular hood and air-foil in reducing drift, and to compare drift using two nozzle sizes.

2. FUNDAMENTAL DRIFT PROCESSES AND LITERATURE REVIEW

A number of research projects have addressed the problem of agricultural chemical drift. The drift process, and possible drift remedies, have been examined at all stages, as outlined in Table 1.

Table 1. Drift Stages

STAGE	IMPORTANT FACTORS
droplet discharge	nozzle size nozzle pressure
droplet transport	meteorological conditions droplet size and spectrum
droplet deposition	wind shear type of target surface

When a pesticide is atomized by a nozzle and released, it has four possible fates. A droplet can land on the intended target, land on the spraying equipment, partially or completely evaporate, or be carried by the wind (i.e. drift) away from the intended target. Droplets which land on equipment do not pose a threat to nearby crops, and may or may not be subsequently wiped onto the target crop. Evaporating droplets pose no threat, but represent a loss of efficiency. To maximize efficiency and minimize risk, the goal of the ideal spraying operation is to release non-evaporating droplets which land immediately on the target.

2-1 Discharge

In the discharge stage, the primary consideration is the type and size of nozzle used to apply the chemical, and the nozzle pressure. Larger nozzles (larger orifice size) and lower pressures produce larger droplets, and smaller nozzles with higher pressures produce smaller droplets. The droplet spectrum from a given nozzle consists of a bell-shaped distribution of sizes from coarse (>400 μm) to fine (<100 μm) droplets. The term ***volumetric median diameter*** (VMD) designates the droplet diameter above which fifty percent of the drops (by volume) are represented. Nozzles such as the common flat-fan 8002, with a pressure of 276 kPa (40 psi), produce VMD's of approximately 300 microns (μm, 10^{-6} m). The 800025 nozzle at 414 kPa (60 psi) produces a VMD of around 130 μm. Coarse droplets are desirable because they are less vulnerable to drift, due to faster settling velocities, and less likely to completely evaporate. However, they require higher application rates and more water dilution, according to Miller (1989), and provide less uniform coverage for a given application rate than fine droplets, according to Rogers and Maki (1986). Appleby (1990) has shown that lower application rates of active ingredient are required with fine droplets. Thus, fine droplets lead to higher ***efficacy***, a term referring to the biological effectiveness of chemical application.

2-2 Transport

In the transport stage, meteorological conditions begin to influence the spray droplet immediately after it leaves the nozzle. The primary factors of concern are the direction and speed of the wind, the relative humidity, and the temperature of the air. Wind speed determines whether the droplet will be swept away from its target and how far it will be carried, while wind direction determines whether the droplet will be carried to an undesired area. Relative humidity controls the evaporation rate. Given sufficient travel time, some drops may evaporate completely before landing. The air temperature of different layers above the ground influences the stability of the atmosphere. The atmospheric stability can determine whether drifting spray droplets will be held near the ground surface or allowed to disperse and dissipate. Akesson and Yates (1987) found the ***stability ratio*** (SR) to be correlated to downwind drift. Downwind drift was found to be much greater for low wind-high SR conditions than for high wind-low SR conditions. The SR is given by the following equation:

$$SR = \frac{(T_{10} - T_3) \times 10^5}{U^2} \qquad \text{(Eqn. 1)}$$

where:

SR = stability ratio
T = temperature at 10 and 3 m heights (deg C)
U = average wind velocity between 10 and 3 m (cm/sec)
10^5 = factor to put result into "easily handled units"

With an SR above 1.3, an inversion cap exists (highly stable air) which will confine drifting material. Negative values indicate vertical mixing or turbulence which will encourage droplet dispersion and dissipation. For values between zero and 1.2 the atmosphere is considered moderately stable.

2-3 Deposition

In the deposition stage, a droplet must overcome wind shear forces over the contact surface before landing. Wind shear, the flow of air parallel to a surface, can deflect a droplet on its approach and carry it over the initial destination, such as a plant leaf. The importance of the shear effect varies with the type and size of target. A droplet entering a crop canopy will likely be deposited due to the variety of leaf orientations and density of leaves. A droplet approaching a single flat surface, however, may be carried over and beyond it.

2-4 Technologies for Reducing Drift

Nozzle type, as previously discussed, can be a variable in drift control. Spraying Systems Company recommends its ***FullJet*** and ***FloodJet*** nozzles for applications in which drift is a concern (Catalog 39, 1987). Operated at very low pressures of 69 to 173 kPa (10 to 25 psi), these nozzles produce coarse, less drift-vulnerable droplets exceeding 1000 microns. However, droplets this large are unsuitable for post-emergent crops because they adhere poorly to plant leaves.

The droplet spectrum from a given nozzle is an important consideration. As previously discussed, the smaller droplets in the spectrum are of primary importance where drift is concerned. Winnowing devices, which consist of airstreams impinging on the spray pattern, have been successfully used to remove the smaller, more drift-vulnerable droplets from the spectrum of ordinary hydraulic nozzles (McKinlay, et. al., 1973).

Electrostatic sprayers and wiper rigs reduce drift through a different means of chemical application. With electrostatic sprayers, droplets are charged and attracted to the crop or ground surface (Gebhardt, 1987). An electrical field is generated between the nozzle and the target by ionizing air molecules with a high-voltage pin. The electrical field must be "sufficient to overcome wind, gravitational, and inertial forces that would otherwise cause the spray to miss the target." Wipers employ an arrangement of chemical-saturated rope wicks which come into direct contact with plant leaves (Derting, 1987).

A number of companies offer sprayers or modification kits employing some type of shield or hood to protect droplets from the effects of wind. The Spray Shield[1] (Ag Shield Manufacturing) is sold as an add-on kit, customized for each sprayer. The Spray Shield is a near-rectangular flexible hood covering the boom, with a slight inward curve at the rear. The Wilger Generation II (Wilger Industries Ltd.), Blanchard Auto-fold (Blanchard Rock-a-matic), and Flexi-Coil (Flexi-Coil) sprayers use a "windscreen", a shield made of mesh or perforated material. These manufacturer's claim to achieve the same protective effect as hood of solid material, with the added advantage of visibility for monitoring nozzle performance. The Bourgault sprayer uses "Venturi Design air curtains" to create a protective vertical wall of air around the spray jet. Brandt Industries Ltd. sells Brandt Wind Cones, plastic elliptical cones fitted over the nozzles as a modification. Brandt claims a three-fold decrease in off-target drift.

The Windproof Sprayer, manufactured by Renn-Vertec Inc. of Vermillion, Alberta, Canada, was the focus of this project. Designed by Rogers Engineering, of Saskatoon, Saskatchewan, Canada, the Windproof has a symmetrical metal hood of trapezoidal shape (Figure 1). Along the bottom edge, the hood is 0.78 m (31 in)

---

[1]The use of trade names for commercial products is for informational purposes only and does not imply endorsement of the product named, nor criticism of similar products not mentioned.

wide from front to back. Rogers and Ford (1985) reported that the hood and its front and rear curtain provide a wind-sheltered zone which increases the opportunity for droplet settling. The air-foil mounted on top of the hood is intended to change the air currents such that the back-eddy is eliminated. Thus, the airflow parallels the hood and the ground surface behind it, providing that the sprayer is traveling directly into the wind or at a speed much greater than that of the wind.

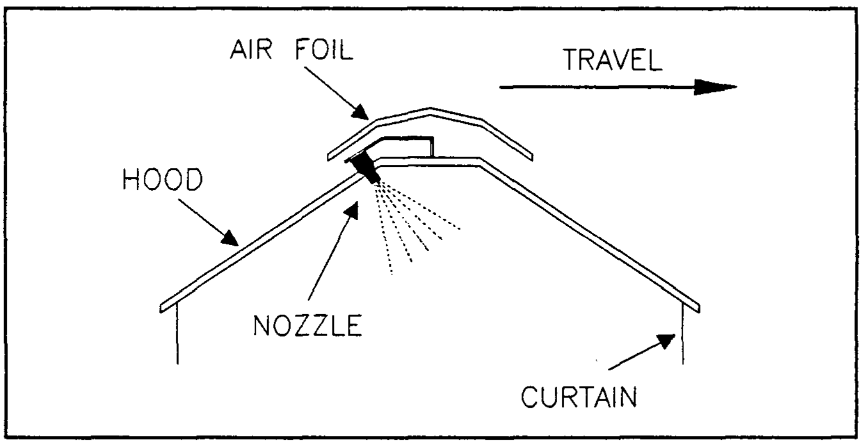

Figure 1. Windproof Sprayer, Side View

2-5 Drift Measurement Techniques

Several means of measuring deposition have been used in spray drift studies. Spray drift collectors have included paper tape, mylar sheets, liquid sensitive dye cards, living plants, monofilament line, and string. The amount of material deposited on these collectors has been determined using visual interpretation, automatic spot counters, colorimetry, and fluorometry. Spray mixtures in drift studies have included fluorescent and non-fluorescent dyes, metallic tracers, and actual herbicides. Table 2 lists common combinations of techniques and equipment.

Table 2. Combinations of Deposition Measurement Techniques and Equipment

COLLECTOR	SPRAY MATERIAL	ANALYSIS METHOD
Paper tape	Dyes, metallic tracers	All methods*
Liquid-sensitive cards	Any liquid	Visual, spot counters
Mylar sheets	Dyes, metallic tracers	Colorimetry, fluorometry
Living plants	Herbicides, dyes metallic tracers	All methods
Line or String	Fluorescent dyes	Fluorometry

* visual, spot counters, colorimetry, and fluorometry

According to Whitney and Roth (1985), wind shear may deflect droplets and carry them over planar surfaces such as paper tape, cards, or mylar sheets. They compared different types of string, monofilament line, and paper tape as collectors of spray drift, hypothesizing that string would increase and stabilize collection efficiency. Rhodamine-B (Rh-B) fluorescent dye and water solutions of varied concentration were sprayed across six-strand mercerized 100% cotton floss and paper tapes, and collection samples were analyzed with a Sequoia-Turner fluorometer. Results indicated a higher fluorescent response and thus increased collection efficiency for the string than for the paper tape.

Salyani and Whitney (1988) compared several water-soluble fluorescent dyes, including Rh-B, Fluorescein, and Uranine, for usefulness in measuring deposition. They found Rh-B to be less sensitive to light and more stable with time than other water-soluble dyes.

2-6 Drift Prediction Model

A computer model in use by the USDA Forest Service and the U.S. Army incorporates spray source information, receptor (target) layout, and meteorological data to predict aircraft or ground spray dispersion and deposition above and within forest canopies (Bjorklund, et al., 1989). The FSCBG (Forest Service Cramer-Barry-Grim, using the initials of its chief developers) model "combines and implements mathematical models for aircraft wake effects, line-source dispersion, drop evaporation, and canopy penetration." FSCBG is comprised of three parts:

1. Simulation of the effects of the aircraft wake on the spray droplets.
2. Simulation of droplet transport and evaporation over open terrain.
3. Simulation of droplet deposition within the vegetative canopy.

Important input parameters include spray droplet distribution, wake type (simple or complex), aircraft (or ground sprayer) characteristics, receptor geometry, source geometry, canopy data, meteorological data, and spray application rate. Program output consists of printouts and graphs, showing deposition versus distance, deposition isopleths on the receptor grid, droplet trajectories, Gaussian ground deposition, droplet diameter versus time, and droplet vertical velocity versus time.

Model assumptions include the following:

1. Flat terrain
2. Line source dispersion
3. Windspeed greater than 0 m/s and positive wind shear
5. Steady meteorological conditions (wind direction allowed to vary)
6. Steady application rates and sprayer velocity
7. Gaussian distribution of deposited droplets

3. OBJECTIVES

The primary objective of this study was to compare the downwind drift under varied wind speeds for the four following sprayer configurations:

A. Conventional open-boom sprayer, 8002 flat fan nozzles, 276 kPa (40 psi)
B. Renn-Vertec sprayer, 8002 nozzles, 276 kPa (40 psi), no air-foil
C. Renn-Vertec sprayer, 8002 nozzles, 276 kPa (40 psi), air-foil
D. Renn-Vertec sprayer, 800025 nozzles, 414 kPa (60 psi), air-foil

Within this comparison, three questions were addressed:

1. Does the hood on the Renn-Vertec sprayer reduce drift? (comparison of A to C)
2. Does the air-foil on the Renn-Vertec sprayer make a difference? (comparison of B to C)
3. How does the drift compare for a smaller drop size? (comparison of D to C)

Proposed wind speed categories were 0 to 2.2 m/s (5 mph), 2.2 to 4.5 m/s (5 to 10 mph), and 4.5 to 6.7 m/s (10 to 15 mph). The goal was to run five repetitions with each sprayer in each of these categories. Other objectives were to determine which meteorological factors contributing to drift, and to find approximate maximum downwind distances at which droplets could be detected.

4. EXPERIMENTAL METHODS

4-1 Field Equipment

Sprayers

Table 3 gives specific information about each sprayer configuration tested. The Rear's sprayer (the control sprayer) was PTO-driven and mounted on a Kubota L2450T tractor, while the Renn-Vertec was pulled by a John Deere 2755 tractor and operated by an ACE hydraulic pump. Sprayer speed was maintained at 9.7 km/hr (6 mph). The Rear's sprayer had a total boom width of 7.3 m (24 ft) with 13 active nozzles at a 0.51 m (20 in) spacing and a height of 0.46 m (18 in). The Renn-Vertec had a 20 m (66 ft) boom with 40 active nozzles at the same spacing and height. The plastic curtain attached to the bottom edge of the hood hung within 15.2 cm (6 in) of the ground surface, which was generally close enough to brush the grass. Three swath widths for sprayer configuration A were equivalent to one swath width for configurations B-D. All sprayers were calibrated to achieve the flow rates shown in Table 3.

Sprayer Tank Mixture

The sprayer fluid, recommended in Barry, et. al, 1978, consisted of a fluorescent tracer and water solution. Rhodamine-B (Rh-B) fluorescent dye, in powdered form, was added to water at 176 mg/l (0.667 g/gal) for configurations A, B, and C, and 1150 mg/l (4.356 g/gal) for configuration D. The increased concentration for configuration D was required to apply an equal amount of active

Table 3. Sprayer Configurations Tested

SPRAYER CONFIG.	TYPE	NOZZLES	PRESSURE kPa	RATE L/min/nozzle
A	Rear's Centrifugal Open-boom	8002 Lurmark Kematol	276	0.757
B	Renn-Vertec RV2350 Air-foil removed	8002 Lurmark Kematol	276	0.757
C	Renn-Vertec RV2350 Air-foil in place	8002 Lurmark Kematol	276	0.757
D	Renn-Vertec RV2350 Air-foil in place	800025 Spraying Sys. Tungsten Carbide	414	0.116

ingredient per hectare. Dye samples were weighed on a Mettler P1200 scale in the appropriate amount for 50 gallons of water, and placed in one liter bottles. At the site, the samples were premixed in the bottles and poured into the sprayer tank. The sprayer was leveled, and water was added directly to the tank through a hose from an irrigation riser and measured volumetrically with the graduations on the front of the tank.

Drift Collectors

The spray drift collectors consisted of 100-foot lengths of string anchored to stakes on each end. The string type was Coats and Clark six-strand "mercerized" white floss. The stakes were 4-foot lengths of 1-inch aluminum tubing driven approximately one foot into the soil. The ends of the string were wrapped around the stakes and secured with rubber bands to prevent slippage. The tension in the string was sufficient to limit sag to less than six inches. The string height above the ground was 0.5 m at the first four upwind and downwind stations and 1.0 m at the other stations.

Weather Instruments

During each sprayer test, four meteorological parameters were monitored. Table 4 summarizes these parameters and the monitoring equipment used.

Table 4. Meteorological Instruments

PARAMETER	NO. OF SENSORS	HEIGHT (m)	EQUIPMENT
Wind Direction	2	5	Sierra/Misco Model 1036HM
		1	Wind Direction Vane
Wind Speed	2	5	Sierra/Misco Model 1036HM
		1	Cup Anemometer
Temperature	2	10	Omega Type T Thermocouple
		2.5	Copper-Constantan
Relative Humidity	1	1.5	Tycos Sling Psychrometer

The wind and temperature sensors were mounted on a tower built for the project from 6-inch and 8-inch aluminum irrigation pipe. The tower was supported by a wooden base and three guy wires at two levels. The wind sensors were mounted on wooden 2-by-2 inch crossarms, fixed to the tower with U-bolts. The crossarms were counter-weighted on one end such that the sensors could be mounted at least six feet from the tower, to minimize any influence of the tower on the wind readings.

A Campbell Scientific CR21X data logger was used to record input signals from both the temperature and wind sensors. Each wind sensor consisted of a cup anemometer and wind vane on a wishbone mount, as illustrated in Figure 2. The wind direction vane used a potentiometer to provide a variable resistance depending upon position. This was incorporated into a voltage-divider circuit, from which the

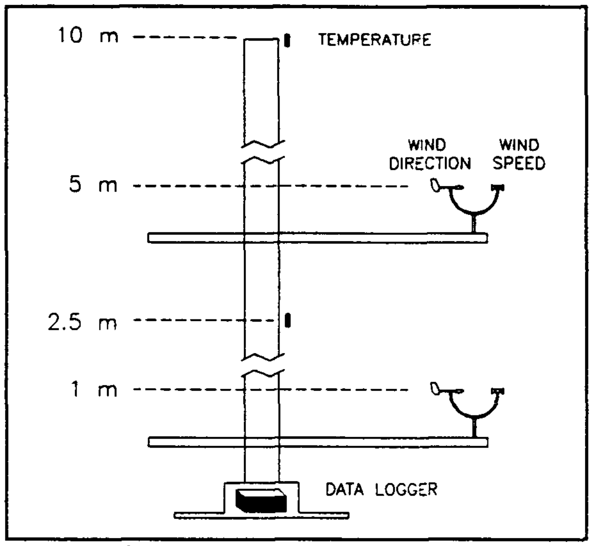

Figure 2. Weather Station

data logger measured the output voltage. The wind speed was measured by the data logger by converting pulses from the anemometer into speed in miles per hour. The thermocouples provided a bi-metal current generation, variable with air temperature, which was detected by the data logger and compared to an internal temperature panel.

The CR21X was programmed to measure wind speed, wind direction, and temperature at one-second intervals and record average values on one-minute intervals. The time (military clock) and the Julian day were also recorded each minute. The data logger was placed at the base of the tower and connected to the weather instruments at the beginning of each trip to the field, and recorded data continuously in memory. The procedure for downloading the data will be discussed in a later section. Instantaneous weather readings could be viewed on the CR21X's display, to help determine suitable times for spraying trials.

The dry and wet bulb temperatures of the sling psychrometer were hand-recorded at the beginning of each test and converted to relative humidity with a psychrometric chart.

4-2 Test Site and Field Layout

The test site (Figure 3) was located 15 miles north of Corvallis, Oregon along the Luckiamute River near the small community of Suver. A field was selected on the W&N Foundation Farm, with permission from farm manager Karl Huber. The field was covered mainly with ryegrass, and bordered by riparian vegetation on the south, west, and east sides. The north side was bordered by a bare, tilled field with an 8 percent uphill slope. The test field itself sloped about 2 percent downhill from

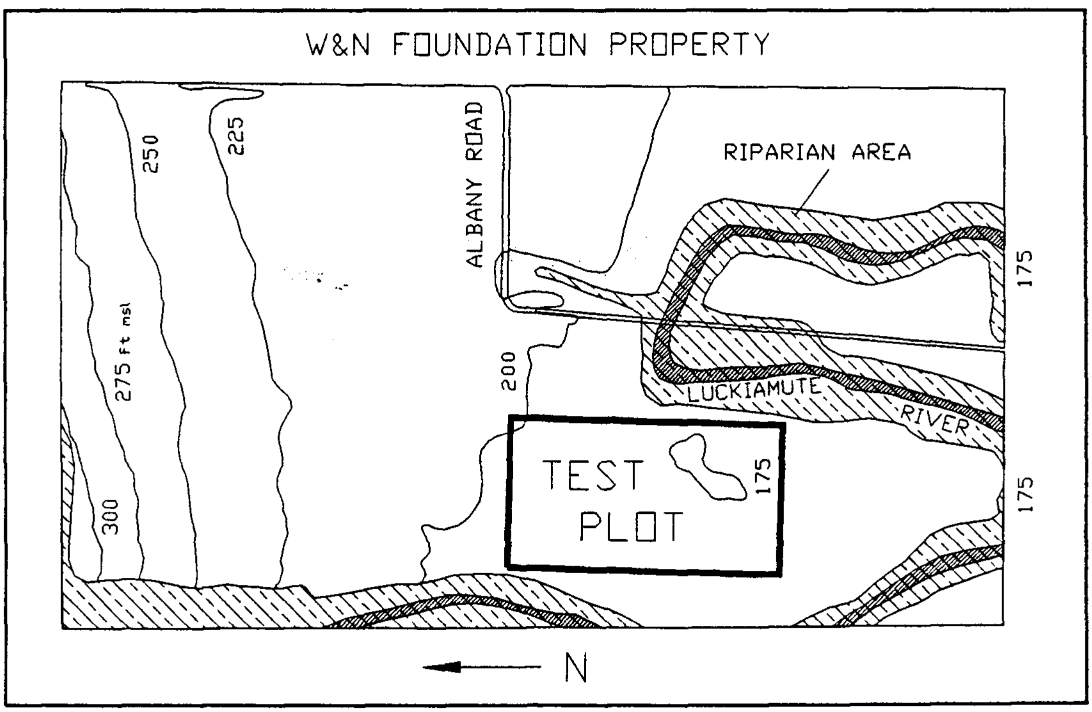

Figure 3. Test Site

the northern edge to the center.

Figure 4 illustrates the layout of the test plot. The layout was designed for the prevailing northerly winds of the region during the summer months. The sprayer swath was paralleled on both sides, upwind and downwind, by a series of 100-ft string collectors, described in section 4-1. The collectors were placed in a geometric series at upwind distances of -1, -2, -4, -8, -16, and -32 m, and at downwind distances of 1, 2, 4, 8, 16, 32, 64, 128, 256, and 347 m. These distances were measured with a cloth tape from the edges of each side of the Renn-Vertec swath. The first four strings on each side of the swath were set 0.5 m above the ground, with the rest at 1 m. The lower height was established to capture those

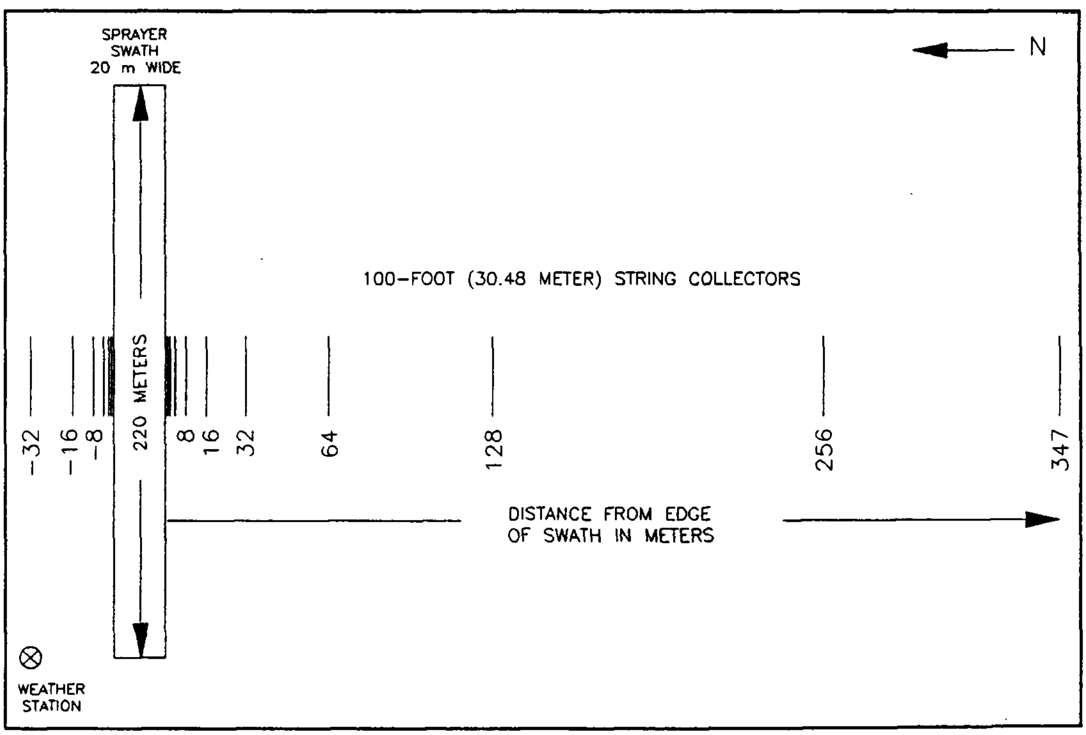

Figure 4. Layout of the Test Plot

droplets escaping the hood near ground-level. The final station was limited to 347 m (rather than 512 m) due to the presence of tall weeds and old hay piles further downwind.

The length of the path over which the sprayers operated was based on the acceptable angle of wind variation (15 degrees), the length of the parallel string collectors (30.48 m), and the downwind distance to the last collector (347 m).

$$\text{PATH LENGTH} = 30.48 + 2(347 \times \tan(15^\circ)) = 216.44 \text{ meters} \qquad \text{(Eqn. 2)}$$

The calculated path length was sufficient to assure that in a wind 15 degrees off the perpendicular, the entire length of string would be exposed to drifting droplets.

4-3 Field Procedures

Sprayer tests were run only under appropriate wind conditions. Instantaneous wind conditions were checked on the data logger. When the wind direction was within 15 degrees of north <u>and</u> when the windspeed was in a category with remaining repetitions, a test could be run. While one person operated the tractor and sprayer, the other recorded the starting and ending time and relative humidity, and monitored the wind conditions. For configurations B-D, the sprayer was operated down and back one time along the path to increase the application rate, and to prevent potential biases associated with the running the sprayer in one direction. For configuration A, the sprayer was operated down and back three times because of its narrower boom width and fewer nozzles. On each of the three passes, a different portion of the swath width was covered to simulate the full-width coverage of the larger sprayer.

After spraying was completed, ten minutes were allowed to pass to allow time for droplet settling. The string samples were then collected for all sixteen stations and placed in pre-labeled plastic bags. The labels indicated wind category, sprayer configuration, and repetition number. New strings were installed as old ones were collected, by simply unrolling and exposing new string from each roll and cutting off the old string from the end.

Great care was taken to prevent contamination of the strings and exposure of fresh samples to sunlight. String rolls were kept in large plastic bags. Hands were thoroughly washed after handling of the dye or dirty equipment. String samples in the baggies were immediately placed in a opaque box.

After each fill of the sprayer tank, spray solution samples were extracted from the tank. These samples were later analyzed to determine the dye concentration, so that adjustments could be made for accurate comparisons of the test results.

At the end of each day of testing, weather data stored on the data logger were extracted for later use. The extraction procedure began by noting sprayer test starting and ending times as written in the project notebook. The data logger's internal memory was then searched and these time windows were located. Temperature, time, windspeed, and wind direction values for each minute of each test were read off verbally, recorded on cassette tape, and eventually transferred to a computer spreadsheet.

Field data were collected from July 21 to September 29 of 1989. This large span of time was necessary to obtain the desired range of wind conditions. While selecting specific wind conditions for each sprayer configuration, no effort was made to obtain specific temperature, relative humidity, or stability ratio conditions. Tests were designated by a three-character code. The first character was the number 1, 2, or 3, representing the windspeed category. The second was a letter from A to D, representing the sprayer configuration. The final character was a number from 1 to 5, representing the repetition number. Due to budget and time constraints, data collection was suspended prior to testing configuration A in the high wind category, tests 3A1-3A5. A summary of the 55 tests completed and their average weather conditions is given in Appendix A.

Unfortunately, there were few days with sustained winds greater than 4.5 m/s. In order to complete the high wind category for configuration B (tests 3B4 and 3B5), the site was rearranged to accommodate the south winds which became prevalent in late September. This was accomplished by installing new stakes to the north of the swath at distances of 64 and 128 m. Beyond this distance, the north field was being irrigated, so the 256 and 347 m stations were not replicated. Data for these stations were estimated from the averages of tests 3B1-3B3.

In several instances, a test was interrupted after one sprayer pass because the wind speed or direction suddenly changed. The test was then resumed when favorable conditions returned. The elapsed time during the delay was monitored so that weather information from this period could be excluded from consideration during analysis.

4-4 Laboratory Equipment and Procedures

The drift comparisons for the different sprayer configurations were based on the amount of drifting material intercepting by the string collectors. The amount of intercepted material was determined by rinsing the collectors and testing the fluorescence of the rinsewater.

Strings were rinsed by adding 50 ml of distilled water to each string bag. Samples were then kneaded for several seconds and placed on a shaker table for approximately 15 minutes, to increase water absorption and maximize rinsing. Finally, the fluid was squeezed out of the string and poured into labeled 35 mm plastic film canisters for storage.

Rinsewater fluorescence was measured with a Perkin-Elmer 650-10S Fluorescence Spectrophotometer, or ***fluorometer***. The fluorometer exposes a fluid sample in a quartz cuvette (or cell) to light at a selected wavelength. The light excites the fluid's fluorescent particles, which then re-emit light at a different wavelength. The measured fluorescence is a function of the amount of re-emitted light. For Rhodamine-B dye, excitation and emission wavelengths of 546 and 590 nm were used (Salyani and Whitney, 1988), with slit widths of 5 nm. Prior to testing, the fluorometer's digital reading was zeroed with a pure distilled water sample. Calibrations were performed with known concentrations of dye, to link the reading to actual parts-per-million (Figure 5).

A range control on the instrument, with possible settings of 0.1, 0.3, 1.0, 3, and 10, controls the aperture of the light source. For very weak samples, the range

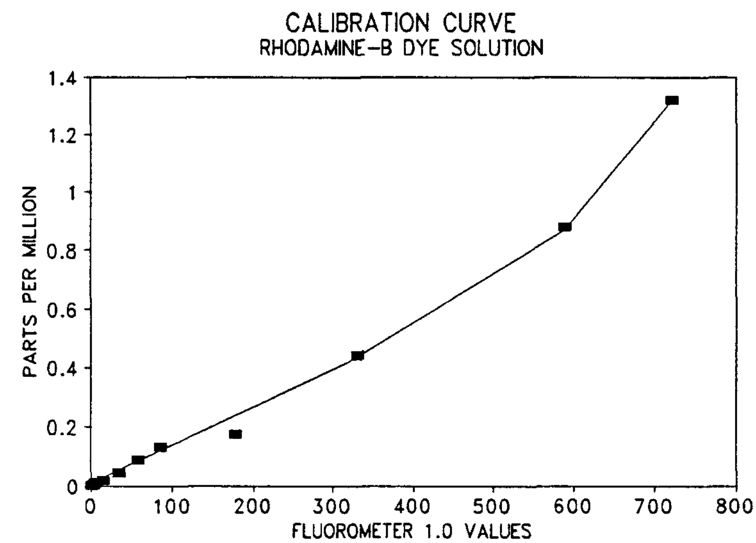

Figure 5. Fluorometer Calibration Curve

is increased to 10 to maximize the aperture. For very strong samples, 0.1 is used to decrease the chance of saturating the detector with too much re-emitted light. The fluorescence as given by the digital reading is a function of the range, such that a ten-fold increase in the range gives a ten-fold increase in the reading. All readings in this study were converted with the following equation to the 1.0 range for the purpose of comparison.

Converted Reading @ Range 1.0 = (Reading @ Range X) / X (Eqn. 3)

Rinsewater samples were tested one at a time in 3 ml quartz cuvettes by rinsing the cuvette with a new sample, re-filling, and inserting it into the cuvette holder inside the fluorometer. The digital fluorescence reading was recorded, and the cuvette was then emptied, rinsed, and filled with the next sample.

Initial observations of fluorometer readings indicated significant amounts of dye downwind (decreasing with distance), evidence of dye on upwind collectors, and higher fluorescence values for configurations A and D.

Two problems were encountered in using the fluorometer. First, the digital readings were seldom steady, varying as much as 10 units after the cuvette had been in place for several seconds. An effort was made to consistently choose the middle point in the range. Secondly, fluorescence values never reached zero. This complicated the task of determining the extent of drift and the true source of the fluorescence (the dye or the string). Tests of clean, unexposed samples of string indicated that some chemical within the string was responsible for 12 to 15 units of fluorescence (1.0 range). Fluorometer values for each collector and test are listed in Appendix B, which also gives fluorometer results for the tank samples.

5. ANALYSIS OF THE DATA

5-1 Preparation

Before any comparisons of sprayer configurations could be made, it was necessary to account for differences in the concentration of the sprayer tank mixtures. The tank samples taken during each day of testing were diluted as necessary and analyzed with the fluorometer (Appendix B). A fluorescence value approximating an average was selected for use as the baseline tank value. Adjustment factors were calculated for all tank mixtures by dividing the baseline by the tank sample value. Fluorometer readings for all string samples were then multiplied by the adjustment factor derived for the corresponding tank sample. Appendix C shows 1.0-range fluorometer readings versus distance from the swath edge for the three wind categories. For these graphs, the zero on the X-axis represents the entire width of the swath. Points on the graphs represent the average fluorescent response for the five repetitions in each category.

It was also necessary to establish a standard of comparison between tests. This standard was termed the ***drift index***, representing the downwind drift for each of the 55 tests completed. The drift index was intended to be an indication of the volume of spray material displaced from the spray swath. Two types of indices were considered. The first was a simple area expression calculated by multiplying the average fluorometer reading for adjacent strings by the distance between the strings, and summing the results for each pair of adjacent downwind strings, as follows:

$$DI = \frac{\sum_{i=1}^{10} \{(f_{i+1} + f_i) * (X_{i+1} - X_i)\}}{2 * 1000} \quad \text{(Eqn. 4)}$$

where:

DI = drift index
i = downwind station number
(i=1 at 1 m, i=10 at 347 m)
f_i = fluorometer reading for string at station i
X_i = distance downwind from swath at station i (m)

NOTE: Divisor of 1000 chosen for convenient magnitude of values

The resulting value was the area under curves of the form shown in Appendix C, excluding the upwind portion and dividing by 1000. The dimensions on this index were fluorescent units times distance in meters; however, the dimensions were ignored and the index was treated as a unitless term.

The second type of drift index considered included an exponent to penalize for downwind drift distance. The equation for this index was:

$$DI = \frac{\sum_{2}^{10} \{X_i^n * (f_i * (X_{i+1} - X_{i-1}))\}}{2 * 1000} \quad \text{(Eqn. 5)}$$

where:

DI = drift index
i = downwind station number
(i=1 for 1 m, i=10 for 347 m)
f_i = fluorometer reading for string at station i
X_i = distance downwind from swath at station i (m)
n = penalty factor (e.g. 1.5, 2)

NOTE: Divisor of 1000 chosen for convenient magnitude of values

This form had the potential to assign a higher drift index to a test in which a small amount of material traveled a great distance, as compared to a test in which a large amount of material traveled a short distance. This potential bias was undesirable, and it was felt that the first form would give a more useful comparison. The chosen drift index was calculated for each of the 55 tests. The results are shown in Appendix D and Appendix E.

5-2 Active Ingredient Calculations

While fluorescence and drift index values were sufficient for comparison purposes, they gave no indication of the actual amounts of material collected on the strings at different downwind distances. Thus, to permit a more practical assessment of the drift control achieved with the hood, these amounts were calculated as a percentage of the in-swath application rate. The procedure follows:

1. Convert 1.0-range fluorometer values to ppm, using the calibration curve, after subtracting 15 units to account for background fluorescence.
2. Determine the total amount of active ingredient (AI) on the string.

$$\frac{(\text{\# parts AI})}{(10^6 \text{ parts soln})} \times \frac{(1 \text{ g/part AI})}{(1 \text{ g/part soln})} \times \frac{(1 \text{ g soln})}{(\text{ml soln})} \times (50 \text{ ml soln}) = \text{\# g AI} \qquad \text{(Eqn. 6)}$$

3. Divide by surface area of string, using 1 mm diameter and 32.81 m length, to determine # g AI/sq m.
4. Find # g AI/sq m applied in swath (same result for all configurations).

$$\frac{(20 \text{ gal soln})}{(\text{acre})} \times \frac{(33.33 \text{ g AI})}{(50 \text{ gal soln})} \times \frac{(\text{acre})}{(4047 \text{ sq m})} = 0.0033 \text{ g AI/sq m} \qquad \text{(Eqn. 7)}$$

5. Find percentage of in-swath application rate by dividing result from 3 by result from 4.

Graphs of these percentages versus distance from the swath are given for each configuration in Appendix F, and will be discussed in a later section.

5-3 FSCBG Comparisons

Drift patterns measured in the field were compared to predictions made by the FSCBG model. Comparisons were based on average fluorescence and weather conditions for the five repetitions in each wind speed category, for each sprayer configuration. No attempt was made to simulate the influence of the hood; the goal was to predict the fate of the droplets upon release from the nozzle, as affected by weather conditions. The actual droplet spectrum escaping the hood was undoubtedly different from that of the nozzles, dominated by smaller droplets. Model inputs are listed in Appendix G. FSCBG graphics output included isopleths of deposit (grams per square meter) over the test plot. Values were obtained from these graphs at the site of each collector, when predicted levels were detectable, and compared to values calculated as described in section 5-2. Comparisons were made in graphs of active ingredient versus distance from the swath (Appendix H), and will be discussed in a later section.

5-4 Modeling Technique

Since weather conditions varied between sprayer tests, direct comparisons could not be made using the initial test results. Instead, the field data were used to develop a model to predict the drift index based on sprayer type and weather conditions. Statistical comparisons were made by analyzing the model's slopes and intercepts. Visual comparisons were made by using the model with a set of synthetic weather data to generate two and three-dimensional graphs.

Prior to modeling, a correlation matrix (Appendix I) was used to evaluate relationships among the weather data, and between the weather data and the drift index. No single factor had a high correlation to the drift index. There were, as expected, strong correlations between the temperature, wind speed, and wind direction at the two elevations. For this reason, later modeling efforts considered only the five-meter wind speed values and ten-meter temperature values. Wind direction values were used only to check for shifting winds and were not used for modeling. There was a strong inverse correlation between temperature and relative humidity, with humidity decreasing with increased temperature.

A multiple regression model was used to determine which of the meteorological factors could be used to predict the drift index for a given sprayer. The first step in the process was to build a table (Appendix J) with the following factors and interactions:

Factors

- sprayer configurations
- relative humidity
- wind speed at 5 m
- temperature at 10 m
- stability ratio
- drift index

Interactions

- relative humidity times configuration
- wind speed times configuration
- temperature times configuration
- relative humidity times wind speed
- relative humidity times temperature
- wind speed times temperature

The rows were filled in with values from the 55 tests. For a test using configuration A, a "1" was entered in the column for sprayer configuration A, while a "0" was entered in the other configuration columns. Thus, columns in this row with configurations B or C times humidity, wind speed, and temperature contained zeroes. The same procedure was followed for configuration B and C tests. Zeroes in the A, B, and C columns implied configuration D tests.

The multiple regression routine was from the StatView 512+ package for Macintosh. Using the table format discussed, the regression compared the drift index values of configuration D to those of configurations A, B, and C. The goal was a linear equation of the following form to predict the DI for any configuration and weather data set:

$$DI = intercept + K_1*RH + K_2*WS + K_3*TEMP + K_4*SR + K_5(RH*WS) + K_6(RH*TEMP) + K_7(WS*TEMP) + RH(K_8*A + K_9*B + K_{10}*C) + WS(K_{11}*A + K_{12}*B + K_{13}*C) + TEMP(K_{14}*A + K_{15}*B + K_{16}*C) \quad \text{(Eqn. 8)}$$

The linear form was chosen to simplify comparisons; there was no reason to believe that a more complex form would be more useful. The first eight terms in this equation were to represent the drift index model for configuration D, with the remaining terms modifying the result for other configurations. The K coefficients were to be derived in the regression process. Again, the values of A, B, and C were to be one or zero, depending upon the configuration.

The routine was initially run with all the listed factors included, termed the full model or zero level. The output from StatView was then inspected and factors and interactions not significantly contributing to the DI (small t value) were eliminated. The process was repeated several times (subsequent levels of model reduction) until nothing more could be eliminated. Removal of factors and interactions was based on the ***extra-sum-of-squares F test*** and a 95 percent confidence level (α = 0.05). The F-statistic for each level was determined according to the equation (Weisberg, 1985):

$$Fstat_i = (RSS_i - RSS_{full}) / (n * RMS_{full}) \qquad \text{(Eqn. 9)}$$

where:

i	=	level
$Fstat_i$	=	level i F-statistic
RSS_i	=	residual sum squares at level i
RSS_{full}	=	residual sum squares for full model
n	=	degrees of freedom (factors or interactions) removed from full model
RMS_{full}	=	residual mean squared error of full model

To validate the reductions at each level, the F-statistic was compared to the table F, F(α, v_1, v_2). For the table F, v_1 is the ***numerator degrees of freedom*** (the n value defined above), and v_2 is the ***denominator*** (full model residual) ***degrees of freedom***. If the F-statistic was less than the table F, the reduction was acceptable at the 95 percent confidence level. A summary of statistical output and calculations at each level is provided in Appendix K.

The model at level 3 was accepted as the final model. The remaining factors were sprayer configuration, wind speed, temperature, and the interactions of wind speed and temperature with sprayer configuration. The final model was represented by the following equation:

$$\begin{aligned} DI = & - 23.707 + 1.171\ WS + 0.899\ T \\ & + \{33.315 - 0.398\ WS - 1.161\ T\} \quad \text{for A} \\ & + \{25.614 - 1.087\ WS - 0.795\ T\} \quad \text{for B} \\ & + \{26.162 - 0.975\ WS - 0.824\ T\} \quad \text{for C} \\ & + 0 \quad \text{for D} \end{aligned} \qquad \text{(Eqn. 10)}$$

where:

WS = wind speed, m/s
T = temperature, degrees C

The constant -23.707 was the intercept for configuration D, and the other constants were adjustments to the intercept for the other configurations. Likewise, the coefficients 1.171 and 0.899 were the slopes of the DI with wind speed and temperature, respectively, for configuration D, while the other coefficients were slope adjustments. In Appendix L, drift index values predicted with the final model were plotted along with observed values for each test.

5-5 Statistical Comparisons

Direct comparisons of slope and intercept from the final model are quantified in Table 5. The DI intercept difference was calculated using a wind speed of zero and a temperature of 15 degrees C, effectively the origin of the data set. The slopes and intercept of configurations B and C showed the only close relationship among these pairs.

A second method of mathematical comparison used confidence intervals given in the StatView output. The upper and lower bounds of the 90 and 95 percent confidence interval are given in Appendix M for each of the final model coefficients. In Figure 6, the 95 percent intervals are illustrated for the coefficients unique to each configuration. The wideness of the intervals can be attributed to the small number of repetitions performed. The 90 and 95 percent confidence intervals overlapped for the sprayer configuration coefficients and the configuration-temperature interaction coefficients. For the interaction of configuration and wind

Table 5. Configuration Comparisons based on Model Equation

COMPARISON	SLOPE DIFFERENCES WS	SLOPE DIFFERENCES TEMP	DI INTERCEPT DIFFERENCE @ WS = 0 m/s, TEMP = 15°C
A - B	0.689[a]	-0.366	2.211
A - C	0.577[b]	-0.337	2.098
A - D	-0.398[a]	-1.161[a]	15.900
C - B	0.112	-0.029	0.113
D - B	-1.087[a]	-0.795[a]	-13.689
D - C	-0.975[a]	-0.824[a]	-13.802

[a] significantly different at 95% confidence level
[b] significantly different at 90% confidence level

speed, the intervals overlapped convincingly only for B and C. The configuration and interaction coefficients for D were all zero by definition, and were not contained in any of the intervals shown.

For two configurations to be equivalent at the 90 or 95 percent confidence level, all corresponding coefficients would need to have overlapping confidence intervals. At 90 percent, the only pair meeting this criterion was the B-C pair. At 95 percent, C overlapped very slightly with A for the configuration-wind speed interaction, suggesting that A and C were the same at this level. However, configurations B and C differed only by the removal of the air-foil, and B did not overlap with A. With additional repetitions, the confidence intervals for all C coefficients would certainly have tightened at least to the width of the B coefficients, eliminating the A-C overlap. Realistically, then, configurations A and D were statistically independent from each other and from B and C, at both confidence levels. The configuration-wind speed interaction was clearly the most

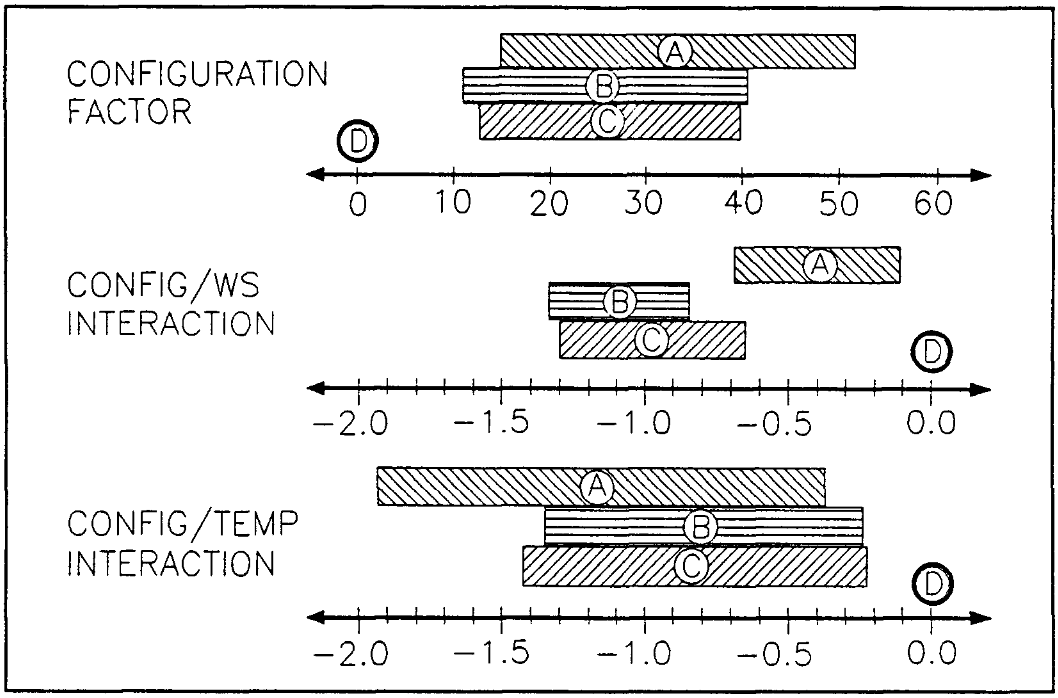

Figure 6. Confidence Intervals, 95%

important factor in separating the DI, since all other A, B, and C coefficients overlapped.

5-6 Visual Comparisons

Visual comparisons of drift for the four sprayer configurations were made by applying the final model to predict the drift index with a set of synthetic weather data. The synthetic data consisted of wind speeds from 0 to 7.5 m/s and temperatures from 15 to 30 degrees C. These ranges were based on the extremes measured in the field. Drift index values were calculated for varied wind speed and constant temperature (Figure 7a), and for constant wind speed and varied temperature (Figure 7b). The constants 3.6 m/s and 22 degrees C were selected from the middle of each range. Figures 7a and 7b show similar DI slopes and intercepts with wind speed and temperature for configurations B and C. Configurations A and D differ in slope and intercept from each other and from B and C.

A three-dimensional representation generated by varying both wind speed and temperature over the same ranges provides the clearest visual comparison (Figure 8). Configurations B and C are shown as nearly parallel planes separated by a maximum of 4 DI units. Configuration A has a negative slope in the direction of increasing temperature, positioned a maximum of 24 DI units above C. Configuration D lies on a much steeper plane with positive slopes, 17 DI units above A at its highest point.

5-7 Error Analysis

An error analysis was performed to evaluate the error associated with drift index values calculated from fluorometer readings. Errors were caused by fluctuations in the fluorometer's digital readout and variations in the background fluorescence of the string. It was assumed that there was no significant error in measuring distances between the string collectors. Calculation of the absolute error in the fluorometer-value DI (δDI) are included in Appendix N. Results are summarized in Table 6. The total of the δDI error terms was $\pm$ 1.60 DI units (3 percent of full scale), small enough for reliable comparisons using the drift index. It was assumed that measurement errors for wind speed and temperature were small and consistent during all tests. Therefore, since the main purpose of the model was comparison, errors in the model drift index (Eqn. 10) were ignored in configuration comparisons and no error analysis was performed.

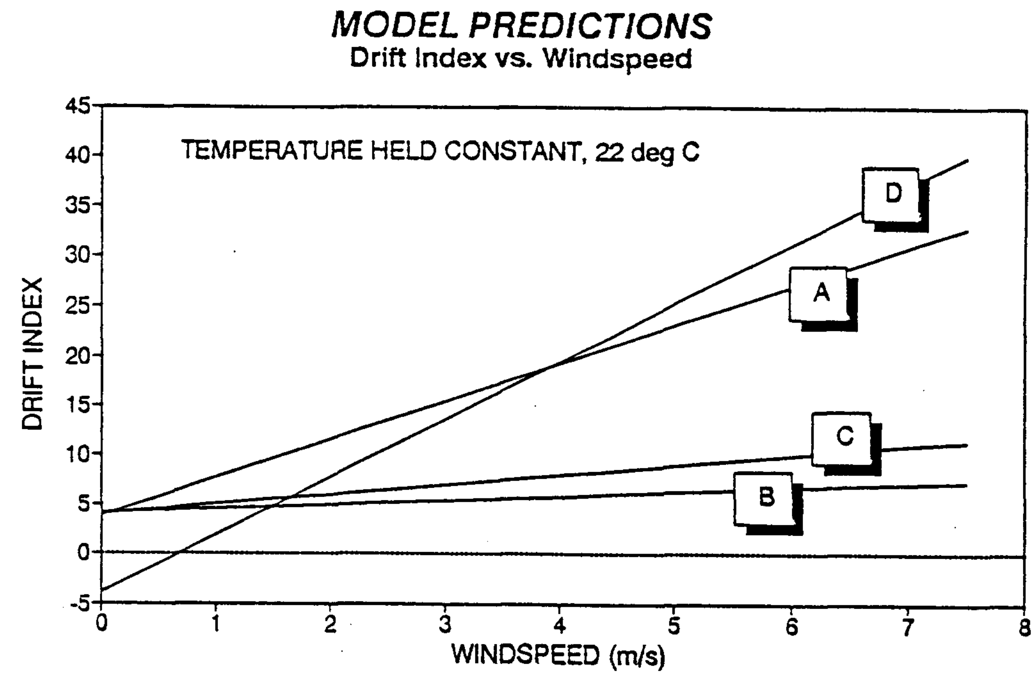

(a)

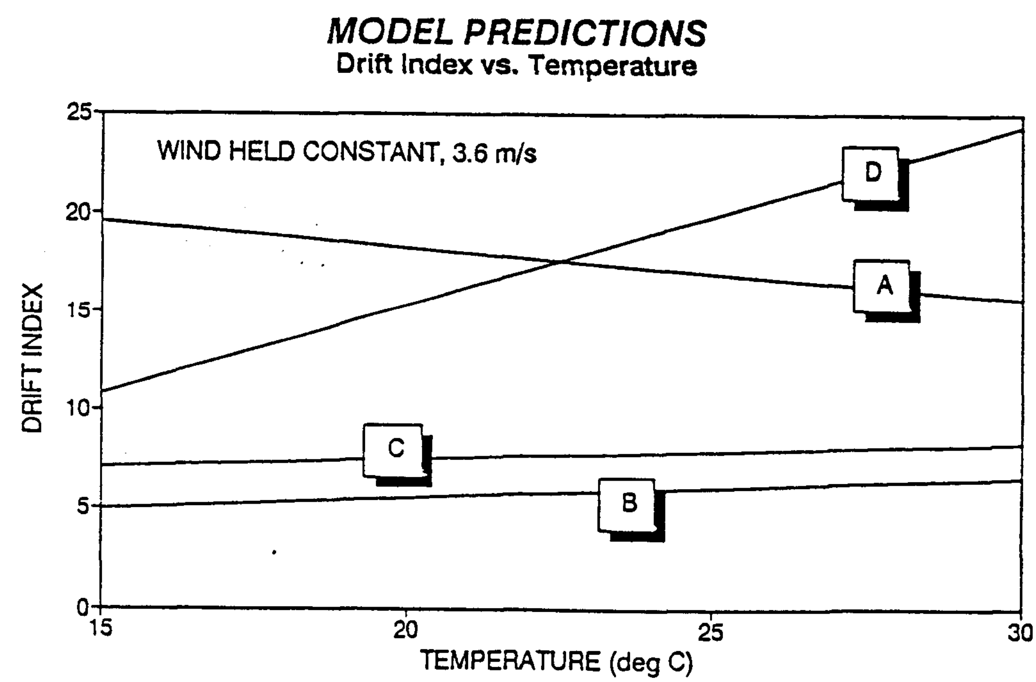

(b)

Figure 7. Model-predicted DI vs. (a) Wind Speed at Constant Temperature and (b) Temperature at Constant Wind Speed

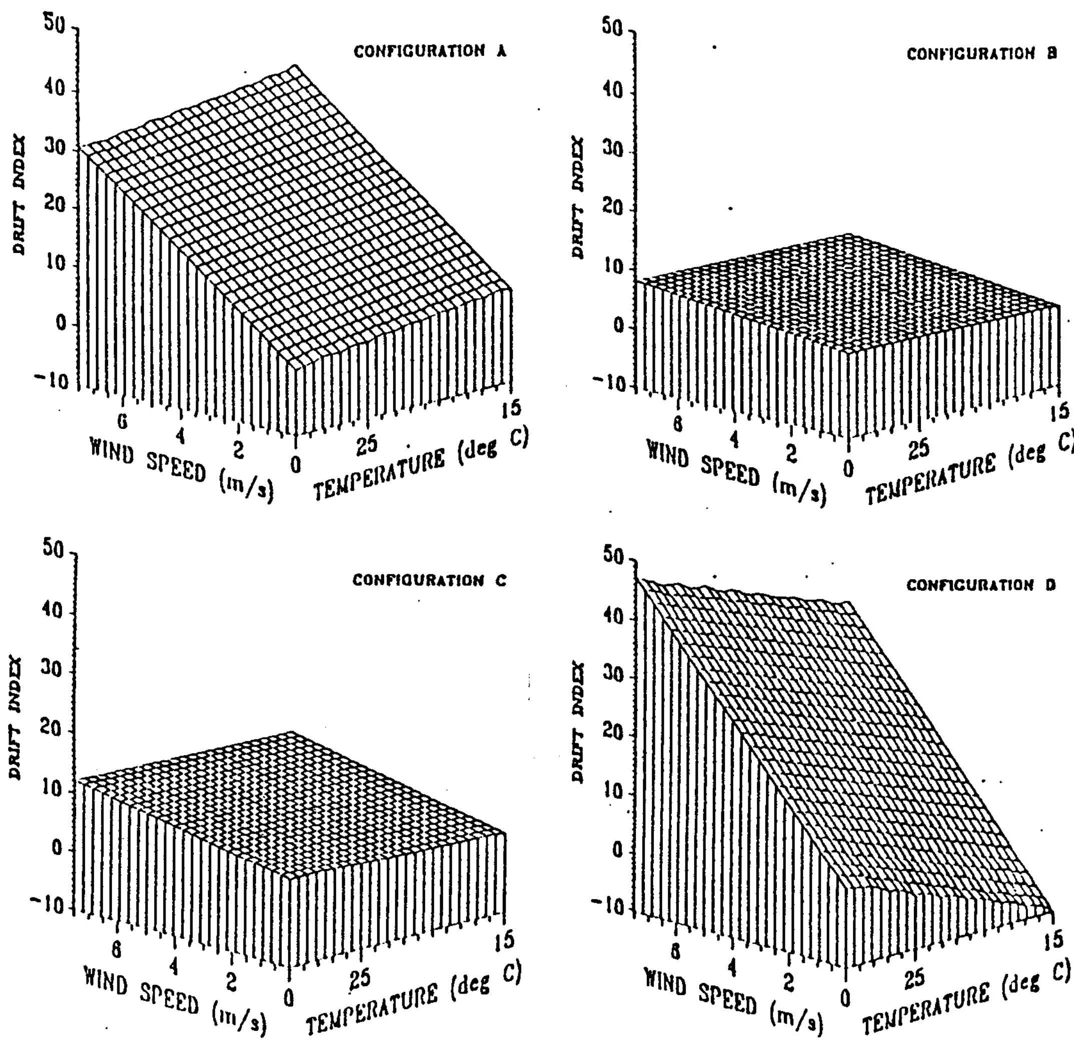

Figure 8. Model-predicted DI vs. Temperature and Wind Speed for All Sprayer Configurations, using Synthetic Weather Data

Table 6. Error Analysis Results

ORIGIN OF ERROR	MAXIMUM VARIATION	MAXIMUM EFFECT ON DI
Readout fluctuations (δf_R)	± 10 units, 1.0 Range	± 1.23
Background fluorescence variation (δf_B)	± 3 units, 1.0 Range	± 0.37

6. CONCLUSIONS AND DISCUSSION

Analysis of the field data provided answers to the questions posed in this research project, as stated in section three. The hood on the Renn-Vertec sprayer helped to decrease drift, while the air-foil had no effect. The use of smaller-orifice nozzles led to significantly increased deposits downwind. The amount of material carried and deposited on the collectors, as represented by the drift index, was influenced primarily by sprayer configuration, wind speed, and temperature. The fluorescent tracer was detected in some tests at the most distant station from the sprayer swath, 347 m downwind. Discussion of each of these conclusions follows.

6-1 Sprayer Configuration Comparisons

Results from section five can be summarized with the following expression, on the basis of maximum drift index values:

$$\text{Configuration B} = \text{C} < \text{A} < \text{D} \qquad \text{(Eqn. 11)}$$

In translation, the air-foil of configuration C provided no apparent advantage in terms of drift reduction over B, in which the air-foil was removed. The hood of configurations B and C led to a significant reduction over the standard open-boom sprayer A. The hood was ineffective, however, in containing the small droplets of configuration D, which had the highest measured and predicted drift index values. Due to slower settling velocities, the small droplets were probably still airborne after the hood passed over, allowing them to be swept away by the wind.

The layout of the field tests directed the wind perpendicular to the boom and the air-foil. This layout may have limited the ability of the air-foil to reduce drift; however, it would be difficult and impractical to always operate directly into the wind, or at a speed much greater than that of the wind. These are the conditions which the design favors. Thus, from a practical standpoint, the benefit of the air-foil is probably minimal.

The benefit of the hood with the larger droplet size was obvious. With the Renn-Vertec sprayer, there were no visible clouds of drifting red dye solution, as was the case with standard sprayer. Data analysis confirmed this observation, showing a significant drift decrease for configurations B and C over A. The study did not include modifications of the hood to determine the importance of the plastic curtain, nozzle placement, or hood shape. Therefore, it is not possible to extend the results to other types of hoods, such as the windscreen designs discussed previously. It seems likely, however, that the openness of the screen design would permit more material to escape.

At the upper end of the wind speed and temperature ranges, configuration D yielded higher drift indexes than both the standard sprayer and the Renn-Vertec with larger orifice nozzles. This is unfortunate from the perspective of efficacy, and clearly demonstrates the need for hood or other modifications in order to contain very small droplets.

6-2 Meteorological Factors and the Final Model

The multiple regression and F-test process selected sprayer configuration, wind speed, temperature, the configuration-wind speed interaction, and the configuration-temperature interaction as the factors most important to the drift index. All relative humidity terms were eliminated, in spite of the fundamental link between evaporation and drift. This may have been due to the high inverse correlation between humidity and temperature, and the fact that the highest temperatures measured in the field coincided with the highest wind speeds and the most vulnerable configuration (D). The stability ratio followed no particular pattern relative to the drift index, and was also eliminated from the model.

With an R squared of 0.948, the regression model fit the field data reasonably well. In making predictions from synthetic data, however, negative drift indexes were generated at low wind speeds for configuration D. This could have been due to the limited number of data points used (15 per configuration), or the choice of a linear model form for possibly curvilinear data.

As seen in Figure 7b, the DI slope with temperature was negative for configuration A and positive for the others. Although all configuration-temperature interaction coefficients were negative in the final model, only in the case of A did this coefficient outweigh the positive base temperature coefficient (0.899). Inspecting the field data (Appendix E), it can be seen that in general, cooler temperatures indeed corresponded to higher winds and drift indexes. It is possible that in this case, relative humidity had its predicted effect, giving more evaporation and less drift at higher temperatures. However, it should be remembered that only ten data points were available for this configuration.

6-3 Drift Distances

Appendices B and C show fluorometer values at the extreme downwind station (347 m) ranging from 13 to 23 for configurations B and C, and from 13 to 58 for A and D. Lab tests showed that chemicals in the string were responsible for as much as 15 units. Therefore, it was felt that values under 15 and perhaps 20 could not necessarily be attributed to dye from the sprayer. Values over 20 were found mainly with the more drift-vulnerable configurations (A and D) and in higher wind speed categories, and it is likely that Rhodamine-B was responsible. Thus, it was concluded that droplets were carried at least as far as the edge of the test plot, 347 m downwind of the swath.

Results of most tests indicated some degree of upwind drift (Appendix C). Fluorometer values were smaller in magnitude than on the downwind side, and unexpectedly increased with distance away from the swath. The most reasonable explanation for this was the presence of up-slope air currents as the ground was warmed by the sun. The field sloped approximately 2 percent downwind. It is uncertain whether this effect would be sufficient to carry material against higher winds, or why deposits would increase with distance upwind.

6-4 Practical Evaluation of Drift Control

Graphs in Appendix F were used to interpret the performance of the hood in reducing drift. Points on these two-dimensional graphs represented collector-site measurements of active ingredient as a fraction of the amount applied over the swath. Values were conservative, since it is unlikely that all fluorescent material was removed from the string during the rinsing procedure. Peak percentages occurred, as expected, at the first downwind station in the highest wind category. Maximum values were 10 percent, 0.8 percent, 1.3 percent, and 20 percent for configurations A-D, respectively. Whether these levels would be significant for actual pesticides would depend upon the chemical. A chemical-dependent standard could be established in which some percent of the in-swath application rate would be deemed unacceptable at a certain downwind distance.

6-5 Performance of the FSCBG Model

Drift patterns measured in the field were compared to predictions made by the FSCBG model (Appendix H). FSCBG overestimated peak values of active ingredient by several orders of magnitude. However, minimum predicted values were typically in the same order of magnitude as minimum measured values, and occurred in the same downwind vicinity. The effect of stronger winds was apparent in the FSCBG predictions, as downwind values increased in higher wind categories for each sprayer configuration. Contrary to measured values, FSCBG predicted lower amounts of ingredient for configuration D (smaller droplets), and expected no material to be deposited upwind of the swath.

7. RESEARCH LIMITATIONS AND PRACTICAL CONSIDERATIONS

This research would have benefitted greatly, time and budget permitting, from additional testing and a broader scope of comparisons. Variables such as sprayer speed and wind direction relative to the sprayer are certainly very important to the performance of a hood design. Removal of the plastic curtain from under the hood would have determined the role of the curtain in reducing drift. Testing of "windscreen" and electrostatic sprayers against the hooded sprayer would have shown which types perform the best. Higher winds, had they been available, would have tested the value of hooded sprayers in very windy regions where conventional sprayers are often unusable. Measurement of the vapor pressure deficit during field tests may have provided the model a more useful parameter than temperature. Perhaps most importantly, more repetitions would have improved the model, and the comparisons made with it would have been even more conclusive.

Limitations of the project require that some conclusions be qualified. The drift detection method used was not applicable to winds blowing directly opposite the direction of travel. Thus, the air-foil was not tested under optimal conditions. All sprayers were operated at 9.7 km/hr (6 mph). The hood would likely have been more effective at slower speeds. Since the main goal of the project was the comparison of sprayer configurations, procedures and equipment were not designed to determine total amounts of drifting material. Material collected on the strings was representative of the component of drift deposited on the ground. The evaporated and dispersed components were unknown.

Ideas for other sprayer modifications surfaced while observing the field tests. A much wider hood would provide increased droplet protection and settling time. The curtain could be custom-made and interchangeable for different crops to improve the hood's seal to the ground or crop. A suction device mounted just behind the back edge of the hood could be used to recover and return any droplets escaping the hood.

Unfortunately, modifications to reduce drift also involve certain trade-offs. Any hardware covering the boom blocks the nozzles from the sight of the sprayer operator, making it difficult to determine whether each nozzle is operating properly. This is especially important when smaller-orifice nozzles such as the 800025 are used. These nozzles became blocked a number of times between field tests, and the only way to determine this was to carefully inspect the swath for gaps in the dye deposits. Flow monitors designed to warn the operator of discharge problems are on the market and may be required with these designs to properly monitor nozzle performance. The additional hardware also makes cleaning and decontamination of the equipment between uses more difficult and time-consuming.

Regardless of the drawbacks, the hood is an effective means of reducing drift and may become the standard of the industry. Continued research and improvements may give more flexibility to farmers in some areas who are currently prohibited from spraying under windy conditions.

BIBLIOGRAPHY

Akesson, N.B. and W.E. Yates. 1987. Effect of Weather Factors on the Application of Herbicides. Methods of Applying Herbicides, Monograph 4, pp. 335-344. Weed Science Society of America, Champaign, IL.

Appleby, A.P. and B.D. Brewster. 1990. Efficacy of Glyphosate Applied with an Air-Foil Shrouded Boom Sprayer. Report to the Western Regional Pesticide Impact Assessment Program. University of California, Davis.

Bjorklund, J.R., C.R. Bowman, and G.C. Dodd. 1989. User Manual: Forest Service Aerial Spray Computer Model - FSCBG (PC). USDA Forest Service, Forest Pest Management, Davis, California.

Derting, C.W. 1987. Wiper Application. Methods of Applying Herbicides, Monograph No. 4, pp. 207-229. Weed Science Society of America, Champaign, IL.

Fehringer, R.J. and R.A. Cavaletto. 1990. Spray Drift Reduction with Shrouded-Boom Sprayers. ASAE Paper No. 90-1008. American Society of Agricultural Engineers, St. Joseph, MI.

Gebhardt, M.R. 1987. Electrostatic Spraying. Methods of Applying Herbicides, Monograph No. 4, pp. 137-144. Weed Science Society of America, Champaign, IL.

McKinlay, K.S., R.J. Ford, and W.K. Martin. 1973. A Means of Winnowing Hydraulic Nozzles to Control Droplet Drift. Canadian Agricultural Engineering, Vol. 15(1): June, pp. 24-26. Canadian Society of Agricultural Engineers, Ottawa, Ontario, Canada.

Miller, Bill. Quoted by Scott Yates in the Capitol Press, March 10, 1989. Salem, OR.

Oregon State University Physics Department. 1984. General Physics Laboratory Guide, pp. 8-9. Corvallis, OR.

Rogers, R.B. and R.J. Ford. 1985. The Windproof Sprayer: Its Progress and Prospects. Agricultural Engineering, Volume 66, No. 11, pp. 11-13. American Society of Agricultural Engineers, St. Joseph, MI.

Rogers, R.B. and R. Maki. 1986. The Effect of Drop Size on Spray Deposit Efficency. ASAE Paper No. 86-1508. American Society of Agricultural Engineers, St. Joseph, MI.

Salyani, M. and J.D. Whitney. 1988. Evaluation of Methodologies for Field Studies of Spray Deposition. Transaction of the ASAE, Vol. 31(2): March-April, pp. 390-395.

Spraying Systems Co., Catalog 39, pp. 14-15. 1987. Wheaton, IL.

Weisberg, S. 1985. Applied Linear Regression, 2nd Edition. John Wiley and Sons, New York.

Whitney, R.W. and L.O. Roth. 1985. String Collectors for Spray Pattern Analysis. Transactions of the ASAE, Vol. 28(6): November-December, pp. 1749-1753.

APPENDICES

Appendix A. Field Test Weather Summary

#	I.D.	RH	WS1 (mph)	WS2 (mph)	TEMP1 (deg C)	TEMP2 (deg C)	STABILITY RATIO	STABILITY CONDITION
1	1A1	0.48	4.747	3.916	25.86	23.17	5.96	inversion
2	1A2	0.58	1.000	1.000	24.79	23.90	44.40	inversion
3	1A3	0.42	3.224	2.821	24.11	22.31	8.66	inversion
4	1A4	0.60	2.139	1.224	18.80	18.91	-1.16	turbulent
5	1A5	0.63	1.000	1.000	18.33	18.16	8.46	inversion
6	2A1	0.45	9.316	7.606	20.55	19.73	0.48	stable
7	2A2	0.44	8.032	6.769	21.22	20.36	0.67	stable
8	2A3	0.62	7.120	6.224	18.70	17.09	1.59	inversion
9	2A4	0.44	7.118	5.852	20.88	20.04	0.84	stable
10	2A5	0.38	8.400	7.046	22.52	21.97	0.39	stable
11	1B1	0.50	4.157	3.043	24.97	25.01	-0.13	turbulent
12	1B2	0.45	1.760	1.414	27.34	27.08	4.31	inversion
13	1B3	0.80	1.164	0.745	15.49	15.71	-7.81	turbulent
14	1B4	0.66	3.062	2.028	22.05	21.79	1.39	inversion
15	1B5	0.50	5.427	4.218	21.08	20.92	0.26	stable
16	2B1	0.61	3.463	2.523	20.50	21.22	-3.01	turbulent
17	2B2	0.45	3.844	2.621	26.54	27.23	-2.31	turbulent
18	2B3	0.80	6.387	4.977	18.28	18.37	-0.12	turbulent
19	2B4	0.66	7.589	6.177	20.29	20.01	0.24	stable
20	2B5	0.56	7.698	6.288	22.67	22.63	0.04	stable
21	3B1	0.56	9.076	7.479	24.30	24.70	-0.24	turbulent
22	3B2	0.62	10.105	7.993	21.33	20.66	0.33	stable
23	3B3	0.62	8.785	6.934	22.08	21.60	0.31	stable
24	3B4	0.71	12.284	9.378	18.01	18.43	-0.14	turbulent
25	3B5	0.63	9.030	6.900	18.82	19.47	-0.40	turbulent
26	1C1	0.78	2.447	1.036	15.24	15.18	0.54	stable
27	1C2	0.65	4.502	3.181	16.16	16.10	0.16	stable
28	1C3	0.48	3.209	1.737	21.35	21.54	-0.94	turbulent
29	1C4	0.71	5.294	3.816	18.61	17.10	2.69	inversion
30	1C5	0.55	5.985	4.541	20.38	18.95	2.00	inversion
31	2C1	0.55	5.478	5.826	20.78	21.43	-1.08	turbulent
32	2C2	0.60	5.420	6.018	22.57	22.68	-0.20	turbulent
33	2C3	0.60	4.487	4.526	22.33	22.80	-1.18	turbulent
34	2C4	0.48	6.655	5.189	25.02	24.57	0.50	stable
35	2C5	0.46	7.849	5.975	25.94	26.18	-0.19	turbulent
36	3C1	0.55	8.983	6.973	21.41	21.85	-0.27	turbulent
37	3C2	0.68	9.142	7.312	17.28	17.47	-0.11	turbulent
38	3C3	0.50	8.536	6.790	25.25	25.53	-0.19	turbulent
39	3C4	0.38	9.741	7.980	22.50	22.64	-0.08	turbulent
40	3C5	0.38	10.205	8.186	22.22	22.13	0.04	stable

Appendix A. (continued)

#	I.D.	RH	WS1 (mph)	WS2 (mph)	TEMP1 (deg C)	TEMP2 (deg C)	STABILITY RATIO	STABILITY CONDITION
41	1D1	0.49	2.237	1.526	23.24	23.07	1.68	inversion
42	1D2	0.28	1.835	1.223	30.47	27.85	38.91	inversion
43	1D3	0.33	2.880	2.388	31.02	29.28	10.50	inversion
44	1D4	0.25	1.520	1.152	34.51	31.70	60.89	inversion
45	1D5	0.35	1.918	1.549	35.74	33.74	27.24	inversion
46	2D1	0.32	5.785	4.656	30.43	29.77	0.98	stable
47	2D2	0.44	7.496	6.306	23.27	21.81	1.30	inv/stab
48	2D3	0.33	6.927	5.977	26.71	25.47	1.29	inv/stab
49	2D4	0.62	7.125	6.179	18.74	16.47	2.23	inversion
50	2D5	0.56	8.406	6.883	19.08	17.94	0.80	stable
51	3D1	0.32	13.096	10.821	27.97	27.48	0.14	stable
52	3D2	0.32	13.354	10.998	29.20	28.60	0.17	stable
53	3D3	0.32	15.695	13.099	29.35	28.70	0.13	stable
54	3D4	0.30	16.809	13.637	29.23	29.02	0.04	stable
55	3D5	0.29	15.814	12.503	29.45	29.29	0.03	stable

								STATION									1989	TANK	ADJUSTMENT
TEST	-32	-16	-8	-4	-2	-1	1	2	4	8	16	32	64	128	256	347	DATE	VALUE	FACTOR
1A1	21.3	12.8	14.5	13.1	13.3	23.0	370.2	251.1	180.0	90.6	67.8	46.4	27.9	13.5	73.4	15.7	Wed 9/20	433.3	0.900
1A2	20.3	14.6	14.0	13.3	12.9	13.9	28.5	18.8	14.1	14.1	12.2	12.4	11.7	10.7	11.1	13.3	Thu 9/21	461.7	0.845
1A3	14.5	11.6	10.7	10.7	10.6	10.7	164.7	93.5	52.1	29.1	19.4	16.9	15.7	11.4	11.8	13.4	Fri 9/22	461.7	0.845
1A4	40.3	35.9	17.8	24.2	29.2	20.8	83.6	47.5	32.8	24.8	21.6	23.7	20.8	17.3	12.3	18.9	Mon 9/25	434.8	0.897
1A5	41.8	24.7	30.1	23.8	28.1	22.7	24.6	18.7	21.1	15.4	19.8	15.5	50.6	41.6	28.4	24.2	Mon 9/25	434.8	0.897
2A1	49.4	33.1	26.5	19.4	24.2	27.1	618.3	442.2	341.9	211.6	216.0	214.7	80.6	48.1	43.0	26.3	Mon 9/18	381.0	1.024
2A2	51.0	38.0	34.5	29.2	32.1	26.5	504.9	353.4	262.9	146.4	95.5	74.6	52.4	27.9	37.7	26.3	Mon 9/18	409.4	0.953
2A3	57.5	34.1	28.0	33.5	34.0	23.1	398.4	284.6	191.8	109.9	66.7	39.8	30.6	30.1	33.8	30.7	Tue 9/19	433.0	0.901
2A4	330.3	79.0	77.5	58.8	54.9	56.1	356.9	257.0	204.2	113.2	86.2	88.3	53.4	34.8	40.8	33.4	Tue 9/19	433.0	0.901
2A5	49.4	34.8	27.5	32.7	27.0	56.6	519.4	380.2	289.2	174.0	123.2	100.3	52.4	36.6	28.4	24.3	Tue 9/19	437.0	0.892
1B1	22.1	19.1	21.9	20.5	17.0	20.0	24.3	27.7	22.8	18.0	17.7	15.3	13.0	14.2	16.1	16.5	Fri 7/28	411.4	0.948
1B2	20.7	21.7	17.1	18.6	16.0	16.1	32.2	23.8	22.3	18.0	16.5	20.9	12.7	15.6	14.0	13.8	Fri 7/28	411.4	0.948
1B3	18.7	12.7	12.5	12.1	9.7	12.4	14.0	11.8	14.7	11.1	12.2	11.4	10.5	10.5	8.5	14.7	Tue 8/8	352.7	1.106
1B4	16.8	14.9	13.2	13.4	11.6	13.5	20.5	16.4	16.6	15.9	14.4	14.4	12.2	13.8	9.2	15.1	Tue 8/8	352.7	1.106
1B5	15.1	17.7	13.6	14.2	12.2	12.6	35.4	27.4	26.9	21.2	20.7	19.5	16.1	14.4	12.7	14.6	Tue 8/8	352.7	1.106
2B1	27.4	34.4	20.7	16.6	17.4	17.1	25.9	30.3	21.7	16.9	18.0	17.4	16.3	14.5	14.9	17.7	Fri 7/28	411.4	0.948
2B2	19.5	19.3	18.2	17.9	15.4	17.6	41.6	35.4	35.2	28.4	25.9	23.0	20.2	15.8	15.5	15.8	Fri 7/28	411.4	0.948
2B3	18.4	16.2	12.5	16.8	11.1	11.7	28.9	20.3	18.4	16.9	13.6	13.5	10.9	12.2	10.6	13.5	Fri 8/4	384.4	1.015
2B4	15.4	12.7	12.1	11.4	10.8	10.5	34.0	28.6	26.5	19.8	19.6	16.0	12.5	12.9	11.3	13.2	Fri 8/4	384.4	1.015
2B5	14.8	13.9	13.0	12.3	35.8	12.8	36.9	27.3	25.6	18.9	16.8	14.5	12.3	12.1	11.9	13.1	Fri 8/4	384.4	1.015
3B1	15.1	25.9	18.6	16.9	19.8	83.3	36.3	32.5	30.3	26.4	23.1	20.6	17.2	15.5	13.5	14.0	Fri 8/4	384.4	1.015
3B2	23.9	21.9	20.9	16.3	16.0	18.3	51.8	49.7	28.6	30.6	26.6	20.8	19.7	18.6	17.4	16.5	Wed 9/27	389.5	1.001
3B3	16.7	18.1	14.2	14.3	24.9	27.0	43.1	46.0	25.2	19.8	19.9	19.4	15.5	16.0	17.9	14.5	Wed 9/27	389.5	1.001
3B4	11.1	9.6	8.9	9.9	13.7	11.8	69.7	55.5	43.1	37.5	21.2	20.0	20.5	17.8	16.3	15.0	Fri 9/29	403.7	0.966
3B5	17.1	12.9	13.9	11.7	17.0	74.6	54.1	41.6	32.4	25.2	21.3	20.4	23.6	22.8	16.3	15.0	Fri 9/29	403.7	0.966
1C1	22.9	15.1	15.1	14.8	13.4	12.1	41.2	31.4	29.9	23.2	19.2	16.7	14.6	13.9	10.2	14.7	Wed 8/9	342.9	1.137
1C2	15.4	17.3	15.1	14.0	17.4	16.3	26.3	20.0	18.8	14.8	15.7	14.6	14.2	15.6	11.4	14.3	Wed 8/9	342.9	1.137
1C3	28.6	17.9	41.1	14.0	15.5	18.4	15.0	14.3	16.7	13.1	15.5	11.6	14.0	13.8	12.4	17.4	Thu 8/24	387.2	1.007
1C4	24.1	25.2	12.9	19.7	18.0	13.5	24.1	18.8	17.4	17.0	21.6	15.9	18.8	13.2	11.0	15.9	Fri 8/25	385.2	1.012
1C5	18.2	17.1	22.2	18.7	19.5	16.7	32.4	29.6	29.7	23.2	19.5	17.5	27.9	21.4	20.5	18.0	Fri 8/25	385.2	1.012

Appendix B. Fluorometer Results from String Rinse Analysis

TEST	STATION -32	-16	-8	-4	-2	-1	1	2	4	8	16	32	64	128	256	347	1989 DATE	TANK VALUE	ADJUSTMENT FACTOR
2C1	30.0	24.1	26.0	21.1	20.7	20.3	42.0	39.4	38.8	30.5	28.0	23.3	23.5	20.4	25.2	19.8	Fri 7/21	328.5	1.187
2C2	35.4	20.3	17.6	17.6	21.5	19.1	61.9	61.7	49.2	38.0	30.3	25.2	22.7	19.1	19.0	20.2	Fri 7/21	328.5	1.187
2C3	22.6	26.8	18.5	18.3	19.4	28.0	92.6	74.2	64.9	50.3	39.8	29.4	25.5	26.1	21.1	18.6	Fri 7/21	328.5	1.187
2C4	17.8	17.5	15.3	15.4	15.3	16.4	43.6	40.0	34.9	28.4	26.2	22.3	16.3	17.0	16.1	14.2	Tue 7/25	328.5	1.187
2C5	19.8	17.7	16.5	15.6	16.7	16.1	70.5	50.5	45.1	36.1	30.5	24.6	18.3	18.4	15.6	13.9	Tue 7/25	328.5	1.187
3C1	19.8	19.9	18.0	18.2	15.8	17.1	44.6	40.4	36.8	30.4	27.3	25.3	19.4	17.7	16.6	16.0	Tue 7/25	328.5	1.187
3C2	15.9	17.7	14.9	14.4	13.4	16.0	67.3	55.5	48.7	33.0	25.2	20.8	19.1	16.6	12.4	14.6	Wed 8/9	342.9	1.137
3C3	16.1	13.7	13.1	12.5	11.2	10.1	60.5	44.3	40.0	28.3	27.0	21.1	17.3	12.5	10.3	14.0	Fri 8/25	385.2	1.012
3C4	67.5	40.8	38.9	32.8	35.2	38.8	109.4	88.3	74.2	58.0	42.2	52.1	34.8	31.6	27.8	23.5	Tue 9/19	374.3	1.042
3C5	36.8	33.4	27.1	28.7	30.3	36.9	96.4	81.5	74.3	55.3	41.6	55.5	35.6	33.6	27.4	23.4	Tue 9/19	374.3	1.042
1D1	25.8	28.5	19.1	26.1	17.6	16.4	175.1	96.2	60.3	43.0	32.0	24.8	19.3	17.0	17.3	21.5	Fri 9/8	270.4	0.991
1D2	32.9	98.3	27.8	25.9	19.8	18.3	196.1	101.8	87.4	50.5	46.8	24.1	24.0	21.5	18.7	30.4	Fri 9/8	270.4	0.991
1D3	43.0	31.1	29.9	29.0	22.1	76.6	238.6	146.2	130.7	96.9	70.7	65.3	45.0	28.2	27.0	23.3	Wed 9/13	286.0	0.937
1D4	47.8	40.9	30.7	26.1	28.1	24.3	121.7	72.8	82.5	49.6	44.4	38.4	31.6	21.7	23.8	26.6	Wed 9/13	286.0	0.937
1D5	37.2	25.8	21.4	22.1	33.3	19.4	273.6	187.2	168.2	118.3	115.9	88.2	63.5	29.4	22.6	19.9	Wed 9/13	286.0	0.937
2D1	64.2	120.3	56.1	60.1	44.7	40.2	273.7	162.1	125.1	107.3	87.0	65.6	50.3	39.2	38.5	34.9	Thu 9/7	281.9	0.951
2D2	44.6	32.7	31.4	25.6	26.7	31.8	206.0	125.4	104.5	69.2	59.7	49.0	39.7	21.3	18.1	22.9	Mon 9/11	267.7	1.001
2D3	58.4	43.1	29.3	37.1	22.4	122.8	247.6	169.2	148.8	103.5	89.3	73.4	64.6	60.4	31.4	22.6	Mon 9/11	267.7	1.001
2D4	76.6	50.9	31.9	28.2	43.3	29.6	242.9	125.3	89.9	55.5	47.0	39.4	35.5	32.4	25.1	27.6	Mon 9/18	233.3	1.149
2D5	49.5	29.1	26.2	23.7	27.4	22.4	440.3	273.9	222.6	141.7	126.6	115.3	67.8	32.0	25.8	26.7	Mon 9/18	233.3	1.149
3D1	40.6	30.1	24.6	29.8	23.4	234.9	752.2	552.3	522.7	360.9	336.1	278.0	174.2	92.6	62.4	41.3	Mon 9/11	267.7	1.001
3D2	70.3	45.0	42.6	242.8	44.9	181.9	848.4	603.7	534.2	426.6	310.4	294.2	197.1	80.4	60.5	38.1	Mon 9/11	267.7	1.001
3D3	53.3	61.0	48.3	73.2	48.1	226.9	858.9	596.1	501.8	366.6	273.3	233.3	166.6	88.6	81.9	46.7	Mon 9/11	267.7	1.001
3D4	165.4	108.3	55.2	67.2	100.6	274.2	882.7	632.2	531.3	412.3	294.2	269.5	200.9	75.5	67.7	48.8	Mon 9/11	267.7	1.001
3D5	120.0	89.4	80.9	58.9	56.3	342.8	848.4	643.7	585.6	440.9	462.8	301.8	174.2	79.0	83.7	57.8	Mon 9/11	267.7	1.001

Appendix B. (continued)

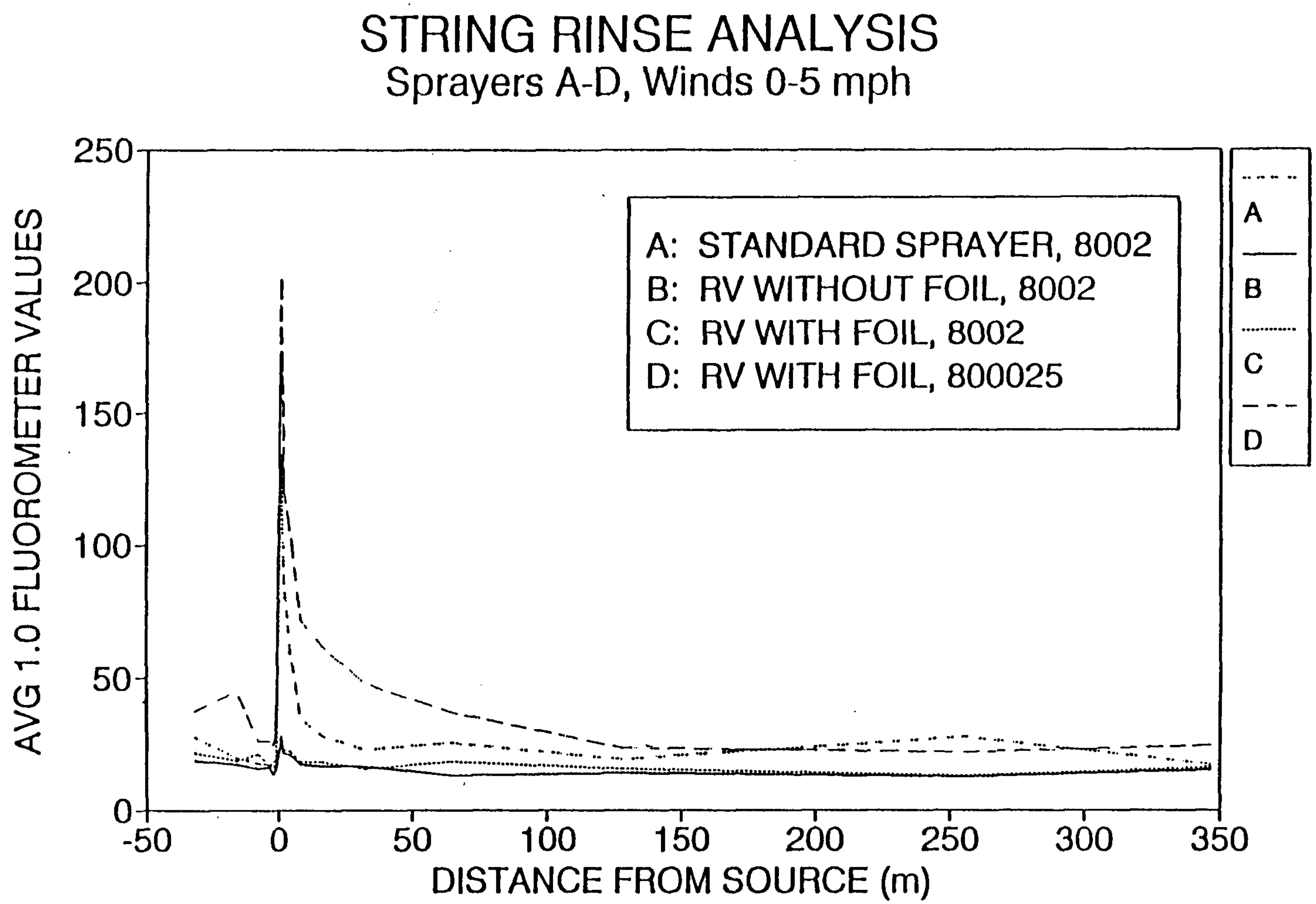

Appendix C. Average Fluorometer Values vs. Distance

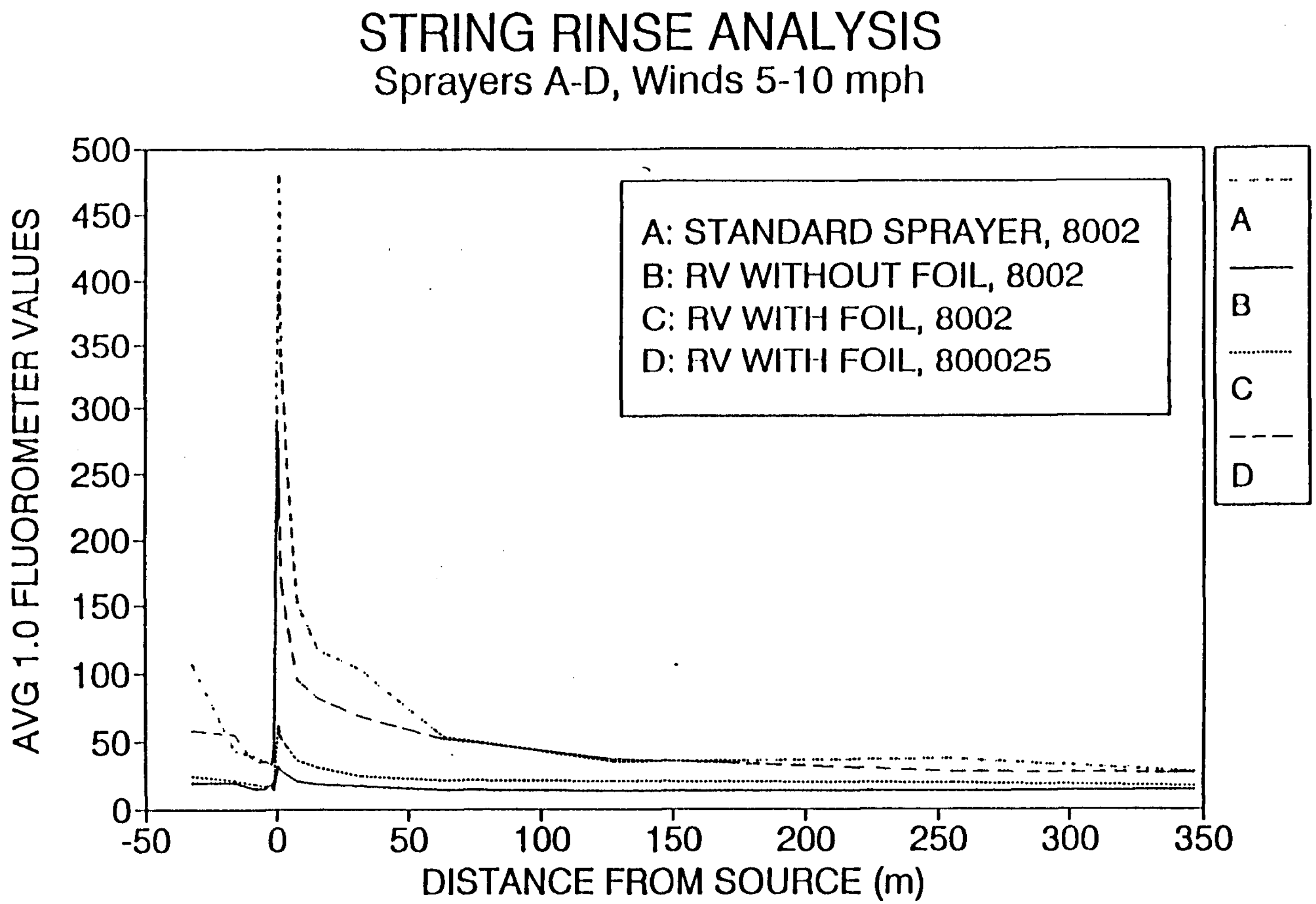

Appendix C. (continued)

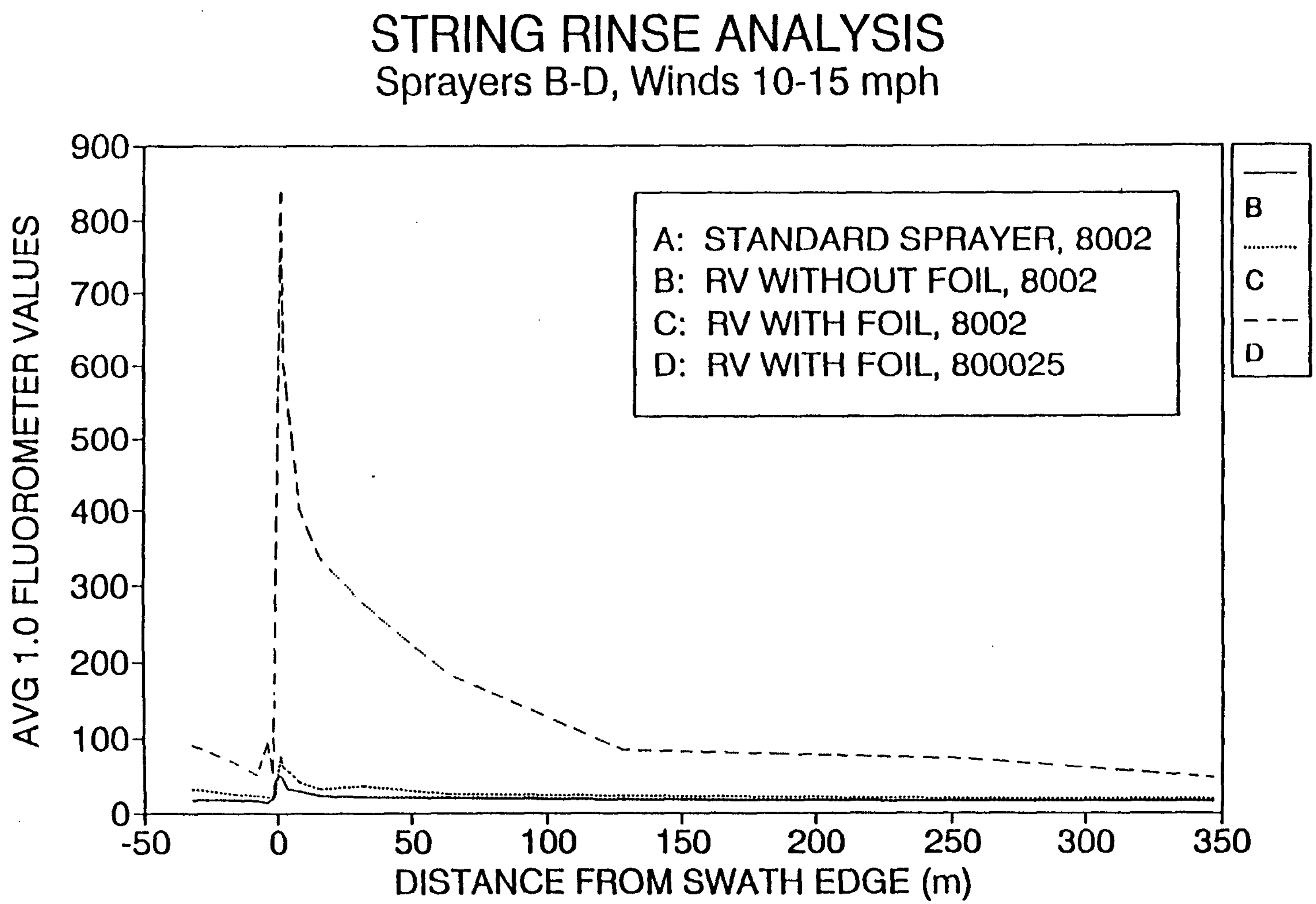

Appendix C. (continued)

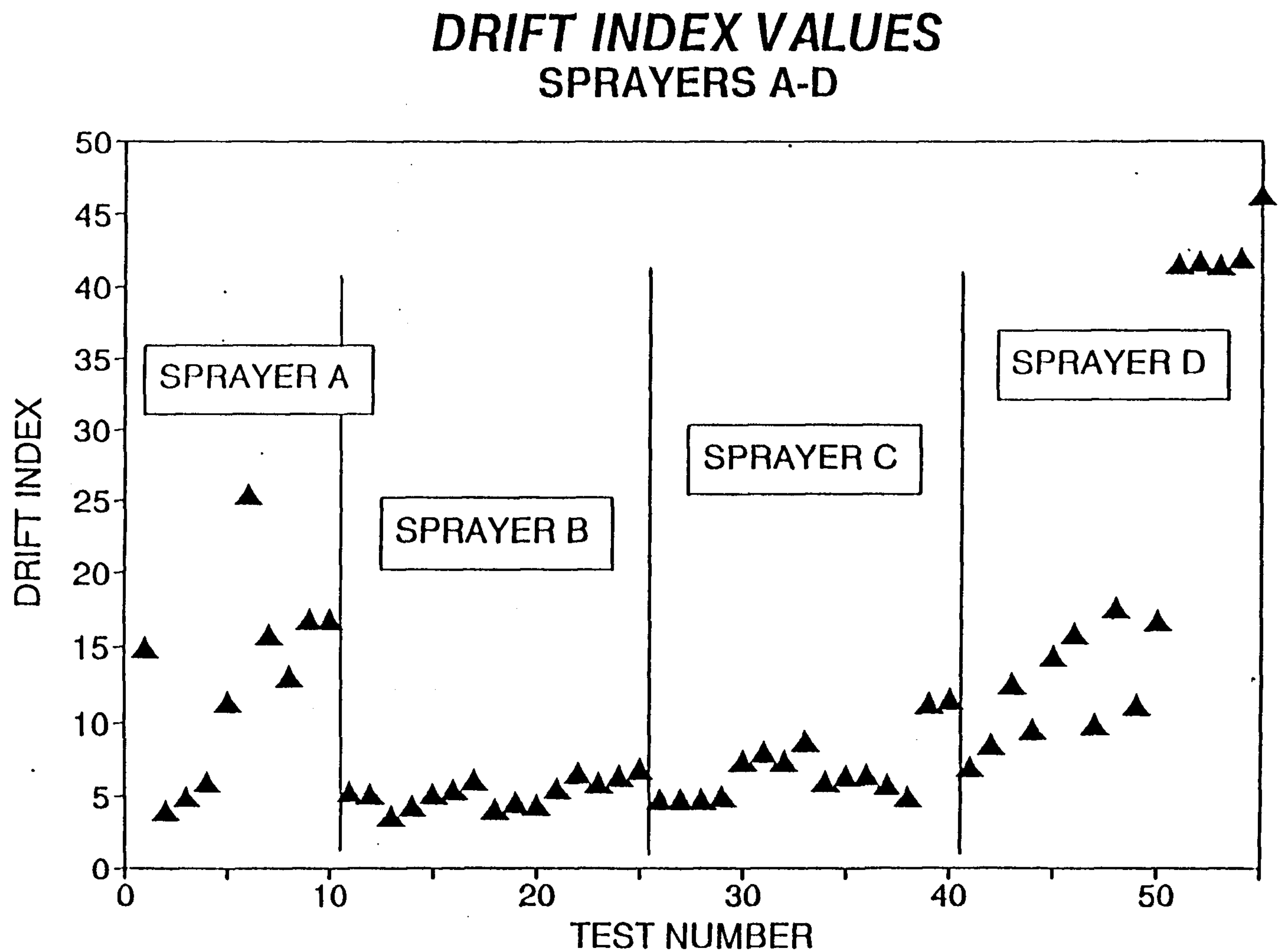

Appendix D. Calculated Drift Indexes for All Field Tests

Appendix E. Field Conditions and Drift Indexes

#	I.D.	RH	WS1 (mph)	WS2 (mph)	TEMP1 (deg C)	TEMP2 (deg C)	STABIL RATIO	DRIFT INDEX
1	1A1	0.48	4.747	3.916	25.86	23.17	5.96	14.96
2	1A2	0.58	1.000	1.000	24.79	23.90	44.40	4.02
3	1A3	0.42	3.224	2.821	24.11	22.31	8.66	4.95
4	1A4	0.60	2.139	1.224	18.80	18.91	-1.16	6.06
5	1A5	0.63	1.000	1.000	18.33	18.16	8.46	11.45
6	2A1	0.45	9.316	7.606	20.55	19.73	0.48	25.40
7	2A2	0.44	8.032	6.769	21.22	20.36	0.67	15.91
8	2A3	0.62	7.120	6.224	18.70	17.09	1.59	13.07
9	2A4	0.44	7.118	5.852	20.88	20.04	0.84	16.90
10	2A5	0.38	8.400	7.046	22.52	21.97	0.39	16.87
11	1B1	0.50	4.157	3.043	24.97	25.01	-0.13	5.31
12	1B2	0.45	1.760	1.414	27.34	27.08	4.31	5.20
13	1B3	0.80	1.164	0.745	15.49	15.71	-7.81	3.67
14	1B4	0.66	3.062	2.028	22.05	21.79	1.39	4.30
15	1B5	0.50	5.427	4.218	21.08	20.92	0.26	5.19
16	2B1	0.61	3.463	2.523	20.50	21.22	-3.01	5.47
17	2B2	0.45	3.844	2.621	26.54	27.23	-2.31	6.13
18	2B3	0.80	6.387	4.977	18.28	18.37	-0.12	4.15
19	2B4	0.66	7.589	6.177	20.29	20.01	0.24	4.55
20	2B5	0.56	7.698	6.288	22.67	22.63	0.04	4.44
21	3B1	0.56	9.076	7.479	24.30	24.70	-0.24	5.52
22	3B2	0.62	10.105	7.993	21.33	20.66	0.33	6.58
23	3B3	0.62	8.785	6.934	22.08	21.60	0.31	5.90
24	3B4	0.71	12.284	9.378	18.01	18.43	-0.14	6.36
25	3B5	0.63	9.030	6.900	18.82	19.47	-0.40	6.87
26	1C1	0.78	2.447	1.036	15.24	15.18	0.54	4.75
27	1C2	0.65	4.502	3.181	16.16	16.10	0.16	4.80
28	1C3	0.48	3.209	1.737	21.35	21.54	-0.94	4.77
29	1C4	0.71	5.294	3.816	18.61	17.10	2.69	4.93
30	1C5	0.55	5.985	4.541	20.38	18.95	2.00	7.40
31	2C1	0.55	5.478	5.826	20.78	21.43	-1.08	8.02
32	2C2	0.60	5.420	6.018	22.57	22.68	-0.20	7.39
33	2C3	0.60	4.487	4.526	22.33	22.80	-1.18	8.73
34	2C4	0.48	6.655	5.189	25.02	24.57	0.50	6.03
35	2C5	0.46	7.849	5.975	25.94	26.18	-0.19	6.40
36	3C1	0.55	8.983	6.973	21.41	21.85	-0.27	6.49
37	3C2	0.68	9.142	7.312	17.28	17.47	-0.11	5.79
38	3C3	0.50	8.536	6.790	25.25	25.53	-0.19	5.01
39	3C4	0.38	9.741	7.980	22.50	22.64	-0.08	11.33
40	3C5	0.38	10.205	8.186	22.22	22.13	0.04	11.56

Appendix E. (continued)

#	I.D.	RH	WS1 (mph)	WS2 (mph)	TEMP1 (deg C)	TEMP2 (deg C)	STABIL RATIO	DRIFT INDEX
41	1D1	0.49	2.237	1.526	23.24	23.07	1.68	7.07
42	1D2	0.28	1.835	1.223	30.47	27.85	38.91	8.60
43	1D3	0.33	2.880	2.388	31.02	29.28	10.50	12.61
44	1D4	0.25	1.520	1.152	34.51	31.70	60.89	9.59
45	1D5	0.35	1.918	1.549	35.74	33.74	27.24	14.40
46	2D1	0.32	5.785	4.656	30.43	29.77	0.98	15.99
47	2D2	0.44	7.496	6.306	23.27	21.81	1.30	9.89
48	2D3	0.33	6.927	5.977	26.71	25.47	1.29	17.64
49	2D4	0.62	7.125	6.179	18.74	16.47	2.23	11.25
50	2D5	0.56	8.406	6.883	19.08	17.94	0.80	16.80
51	3D1	0.32	13.096	10.821	27.97	27.48	0.14	41.61
52	3D2	0.32	13.354	10.998	29.20	28.60	0.17	41.81
53	3D3	0.32	15.695	13.099	29.35	28.70	0.13	41.50
54	3D4	0.30	16.809	13.637	29.23	29.02	0.04	41.98
55	3D5	0.29	15.814	12.503	29.45	29.29	0.03	46.33

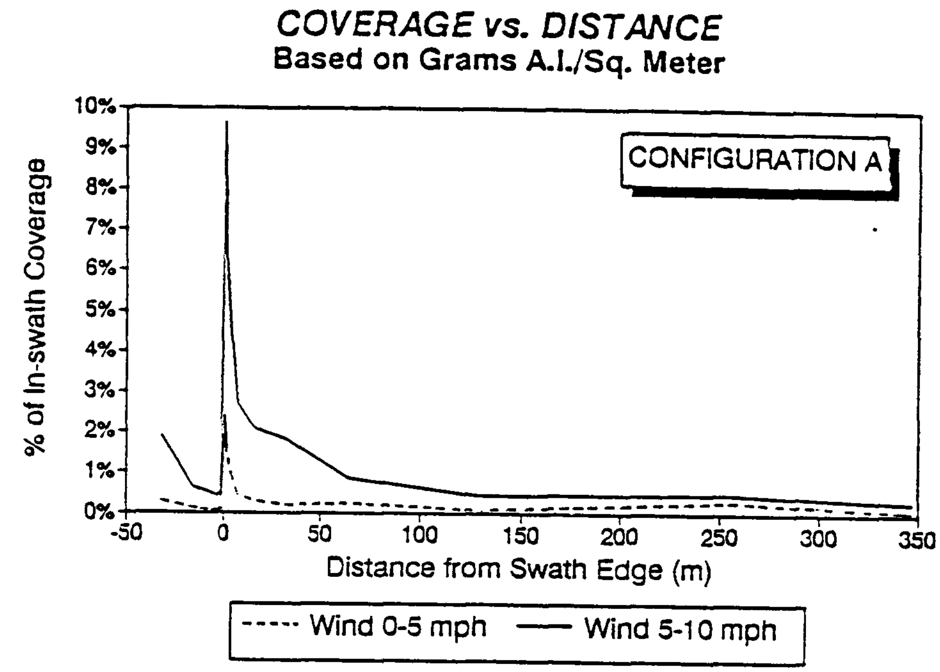

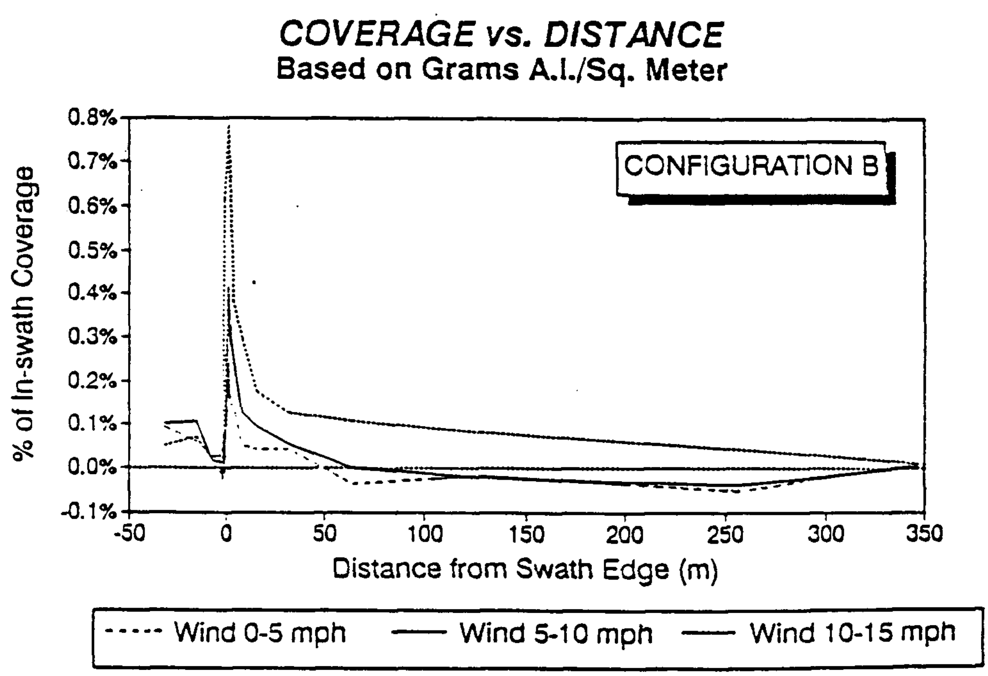

Appendix F. Active Ingredient Collected, as a Percentage

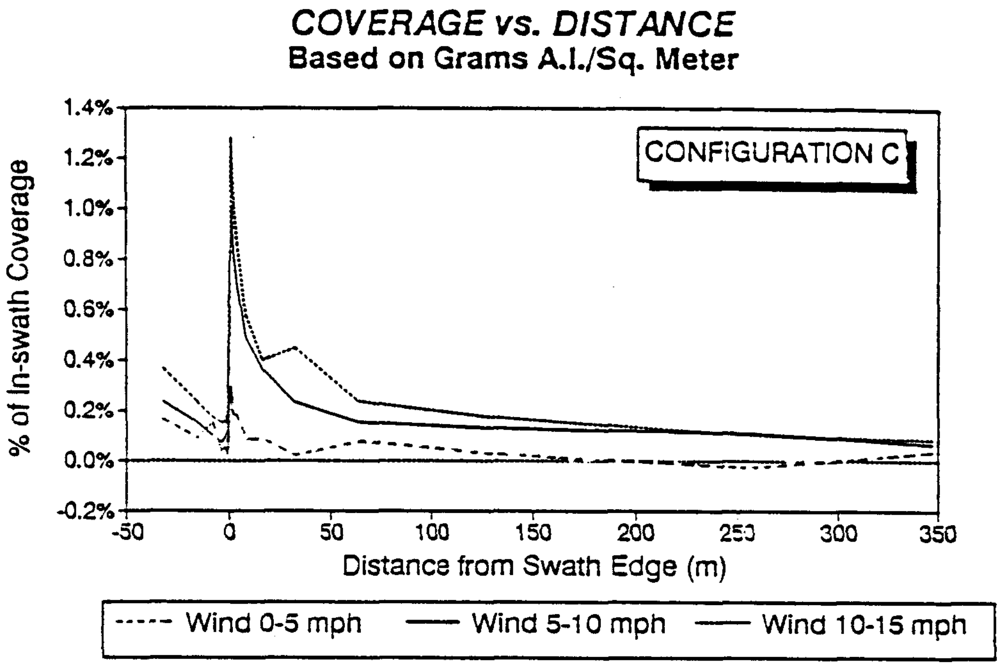

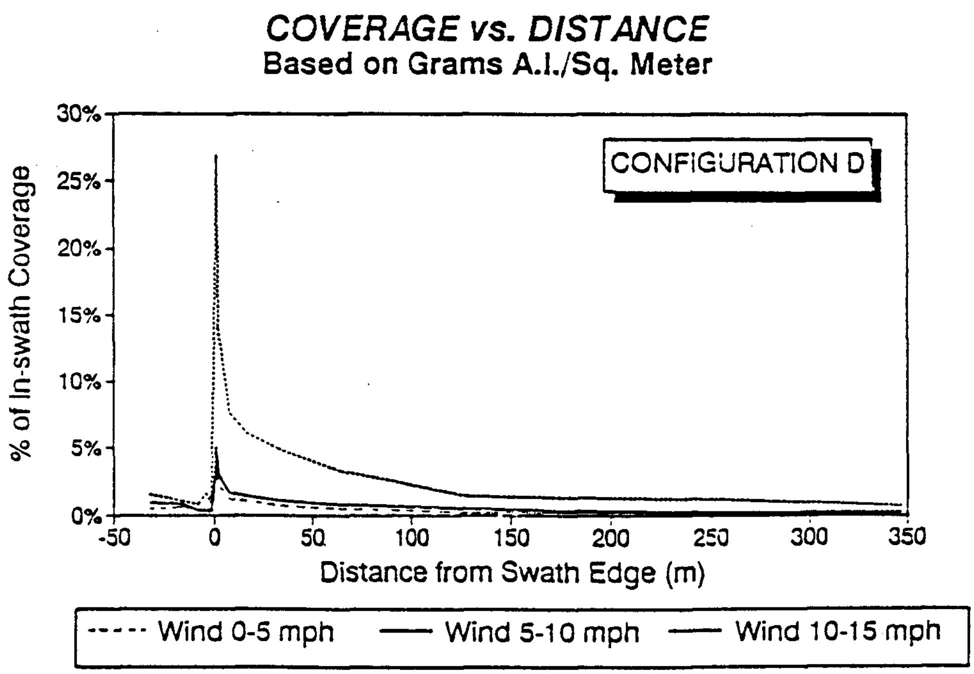

Appendix F. (continued)

Appendix G. FSCBG Program Input

INPUT ITEM	INPUT VALUE OR RESPONSE
Program models selected	no wake, evaporation, concentration and deposition dispersion
Grid system orientation	0 degrees
Grid height	0
Grid X coordinates (m)	-32, -16, -8, -4, -2, -1, 0, 1, 2, 4, 8, 16, 32, 64, 128, 256, 347
Grid Y coordinates (m)	0 to 300 by increments of 25 meters
Flight line sources	1
Height of spray release	1 m
Distance between flight lines	20 m
Emission for each source	20 gal/acre (A, B, C) 3 gal/acre (D)
Wake settling velocity	0.46 m/s
Time to spray cloud stabilization	2.5 sec
Depth of gas sources	1 m
Initial source radius	1 m
Start, end X coordinates of flight line	0 m, 0 m
Start, end Y coordinates of flight line	50 m, 250 m
Spray material	water
Density	1 g/m^3
Spray material half-life	infinite
Average drop diameters	
for A, B, C runs (micro-m)	500, 400, 300, 200, 100, 50
fraction of total volume	.05, .28, .34, .20, .10, .03
for D runs (micro-m)	350, 240, 130, 100, 50, 25
fraction of total volume	.03, .066, .554, .2, .1, .05
Surface pressure	1013 millibars
Net radiation index	1
Observation heights	layer average
Temperature, RH, and wind speed	5 repetition avg for each configuration, wind category
Wind direction	270 degrees
Measurement time for std. dev. of wind direction angle	600 sec

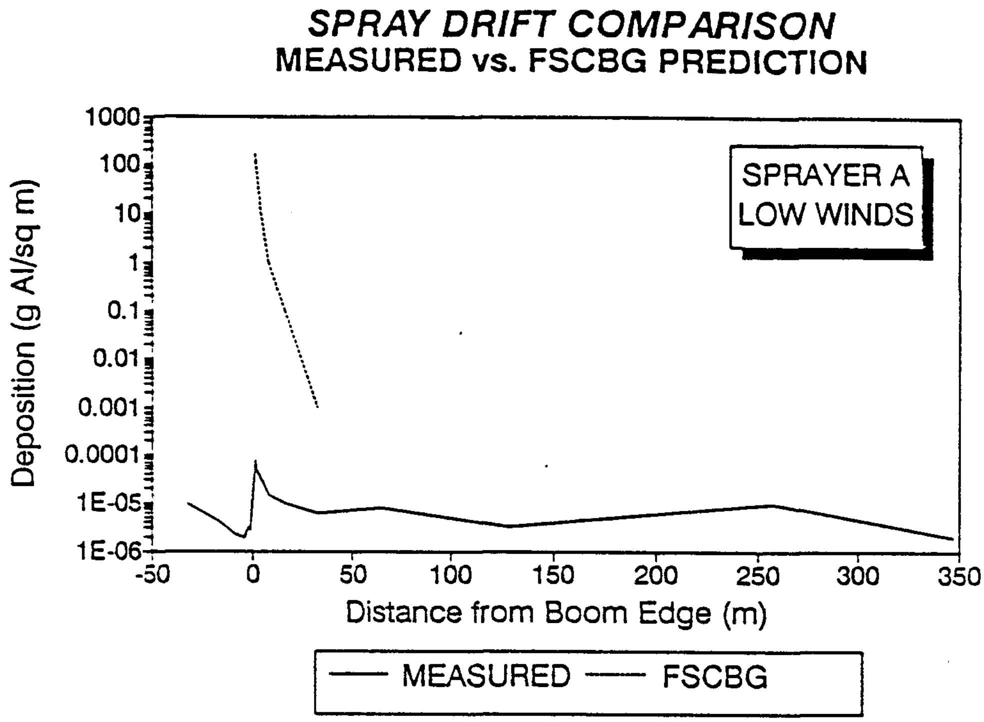

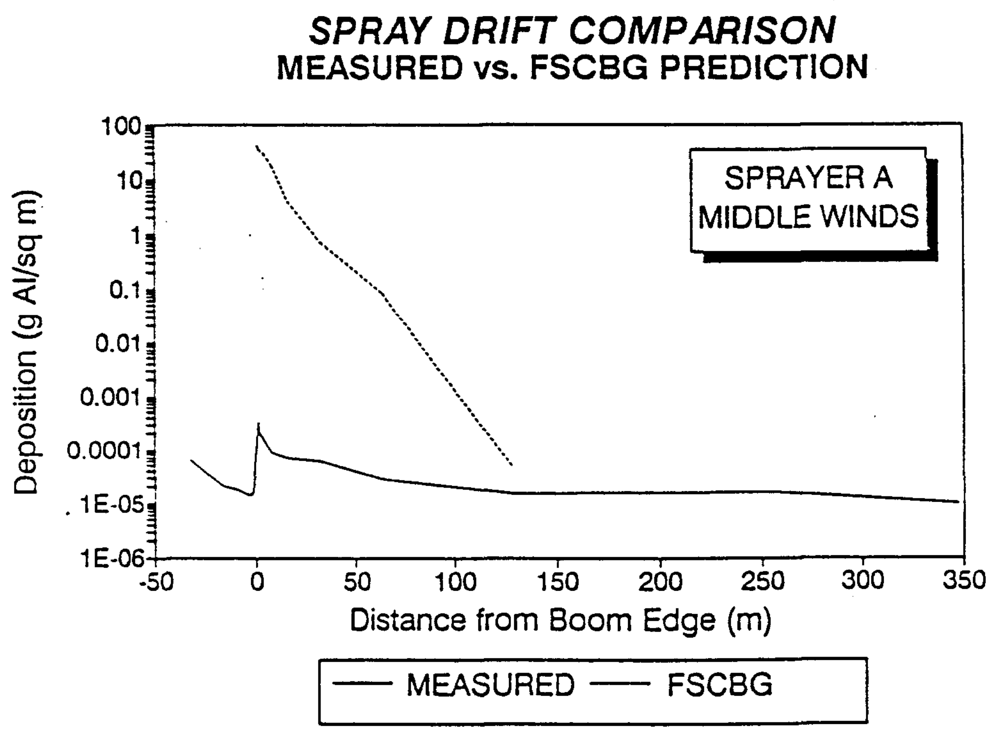

Appendix H. Comparison to FSCBG Predictions

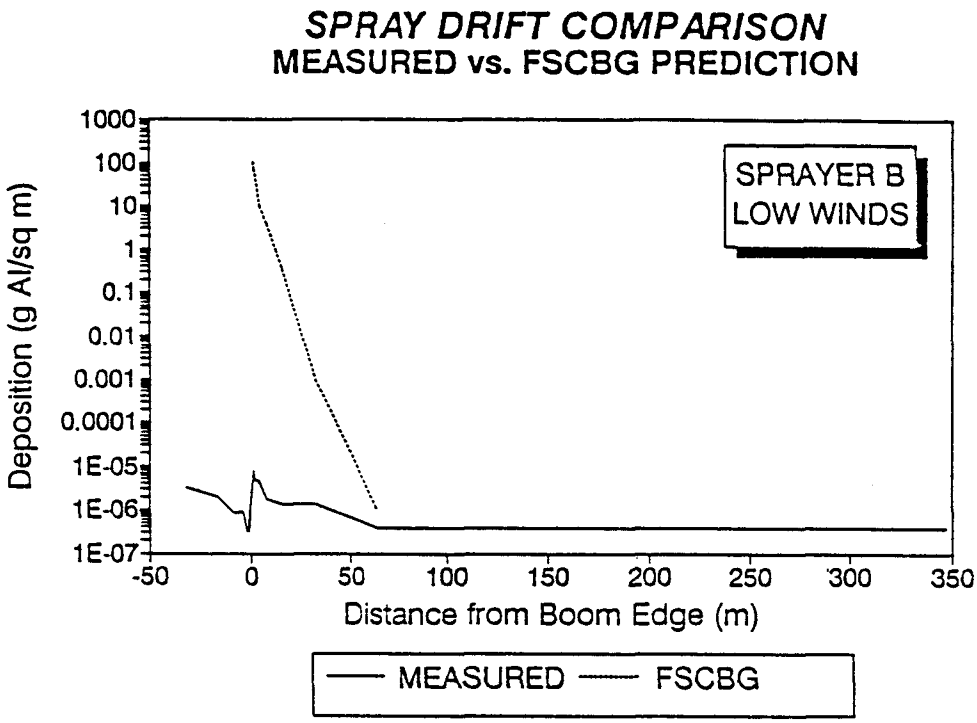

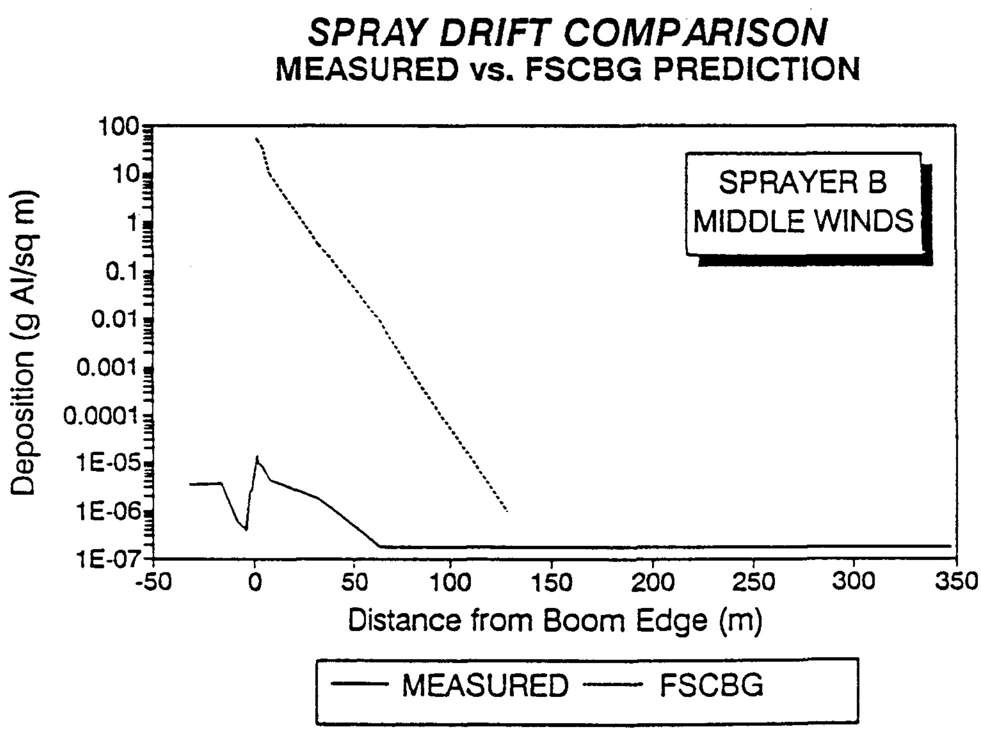

Appendix H. (continued)

SPRAY DRIFT COMPARISON
MEASURED vs. FSCBG PREDICTION

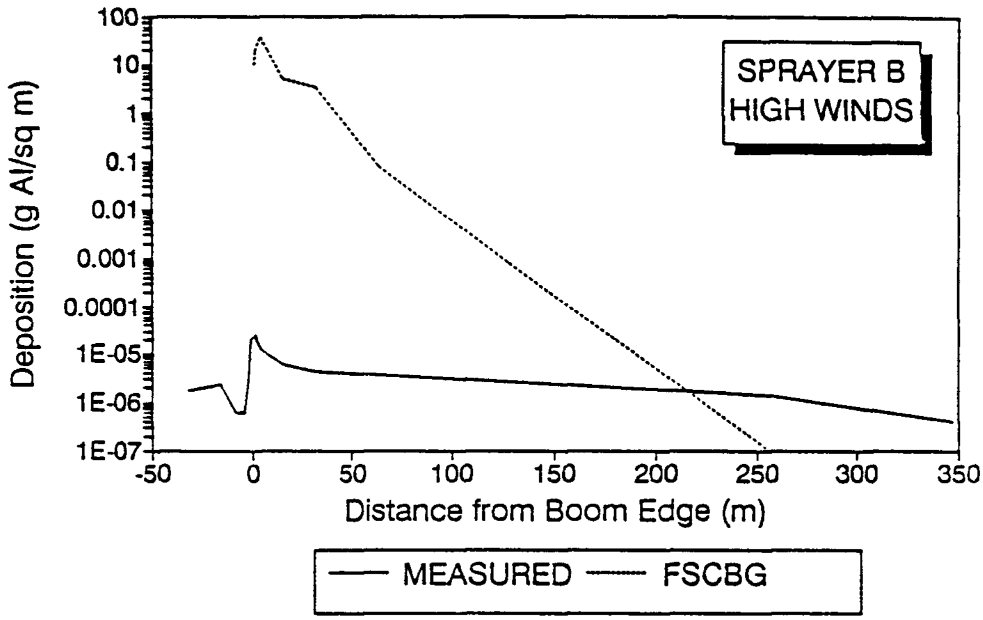

SPRAY DRIFT COMPARISON
MEASURED vs. FSCBG PREDICTION

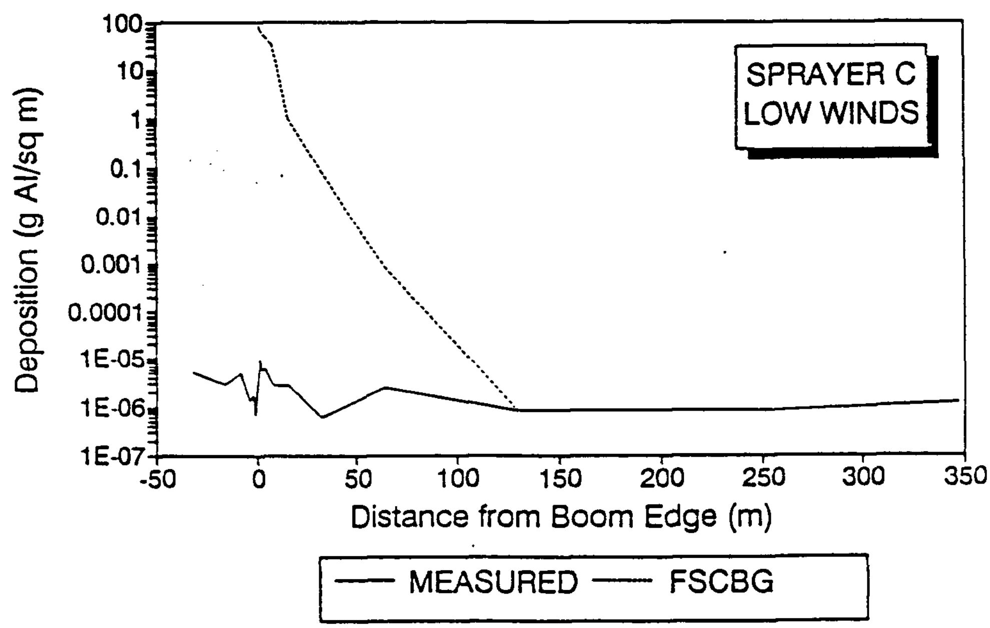

Appendix H. (continued)

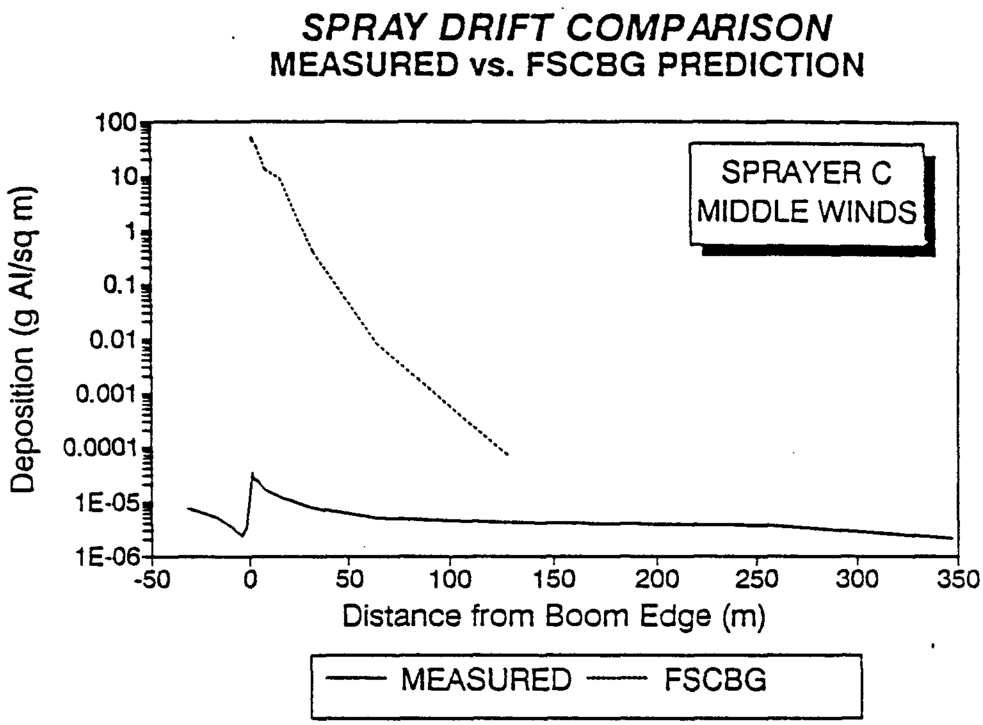

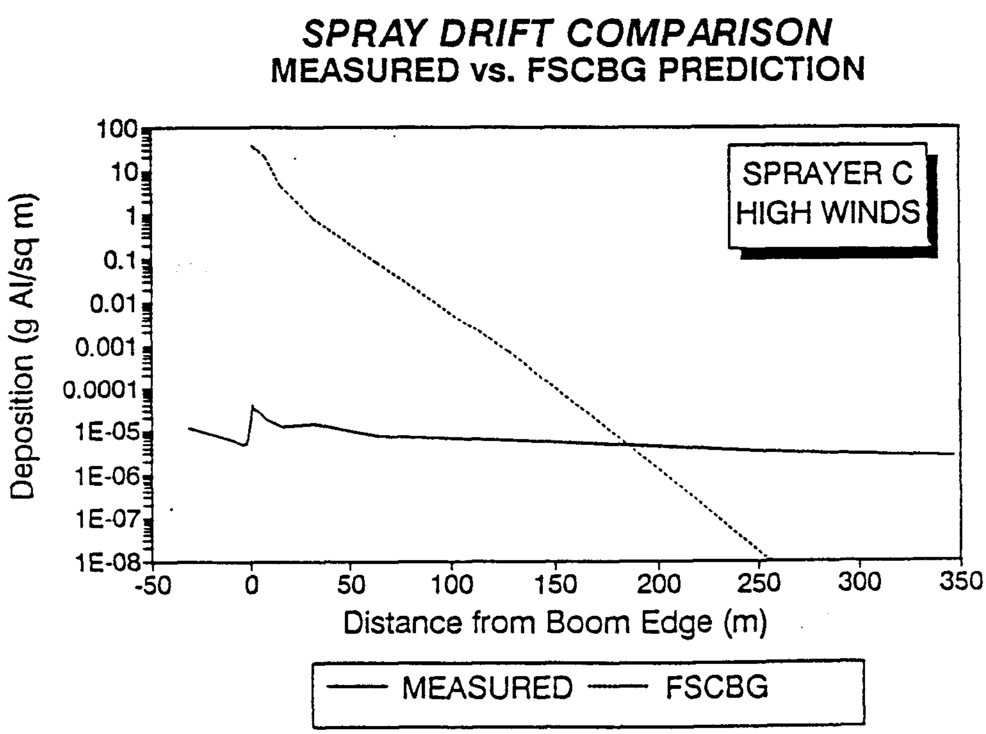

Appendix H. (continued)

SPRAY DRIFT COMPARISON
MEASURED vs. FSCBG PREDICTION

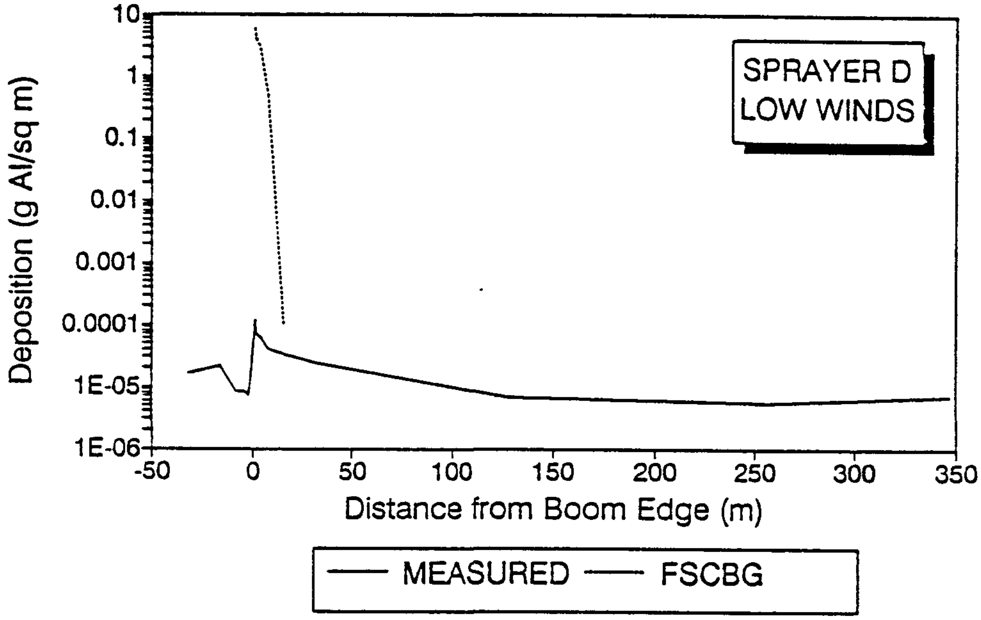

SPRAY DRIFT COMPARISON
MEASURED vs. FSCBG PREDICTION

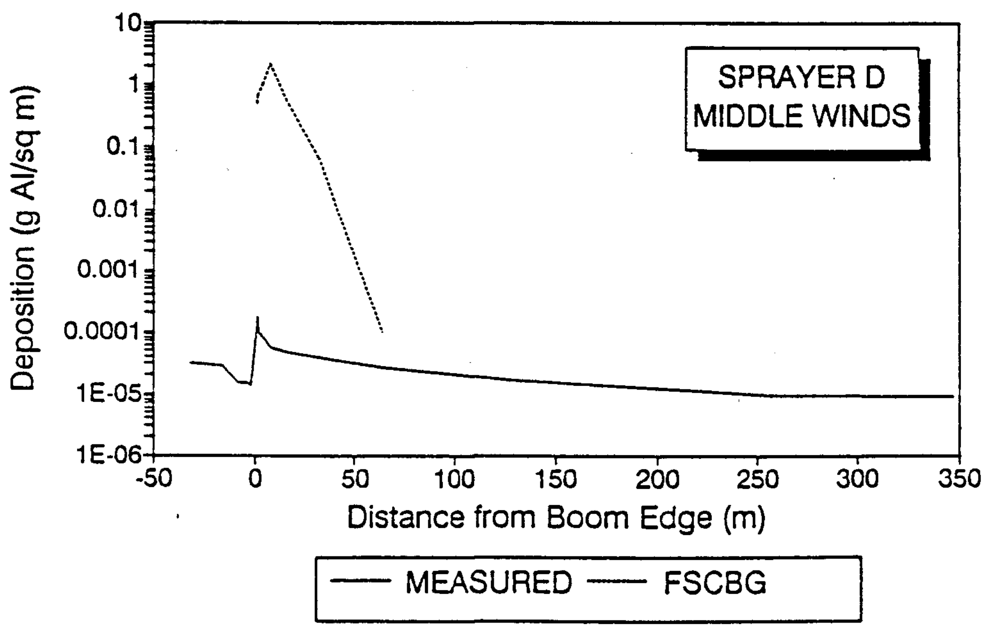

Appendix H. (continued)

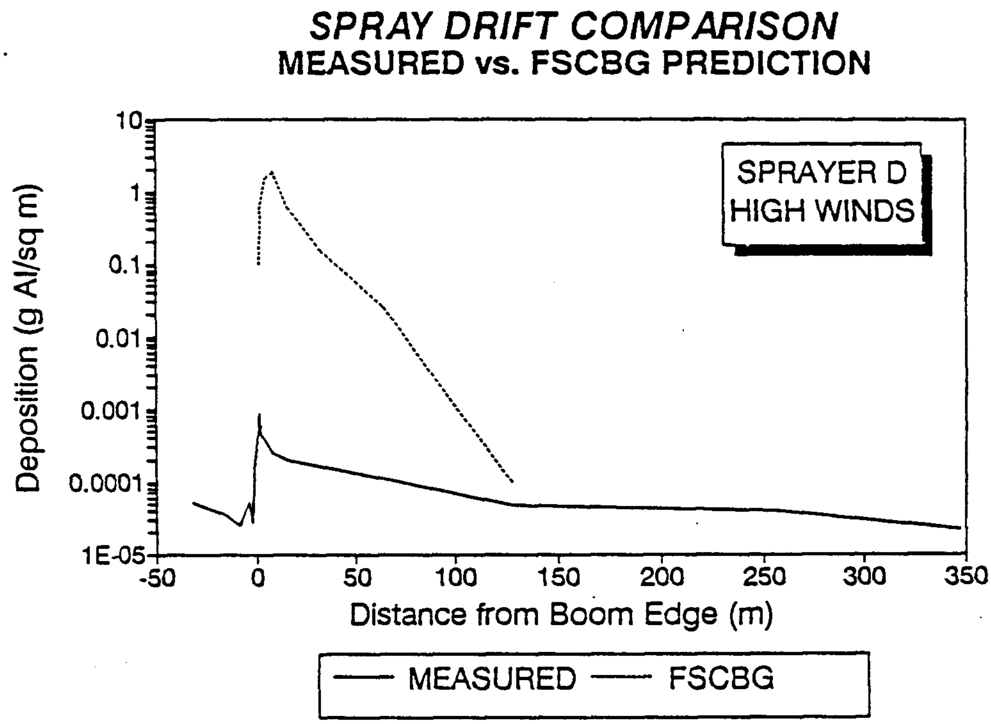

Appendix H. (continued)

	SPRAYER CONFIG.	RELATIVE HUMIDITY	WIND SPEED (at 5 m)	TEMP. (at 10 m)	WIND SPEED (at 1 m)	TEMP. (at 2.5 m)	STABIL RATIO	DRIFT INDEX
SC	1.000							
RH	-0.424	1.000						
WS1	0.245	-0.265	1.000					
TEMP1	0.470	-0.843	0.094	1.000				
WS2	0.246	-0.282	0.991	0.110	1.000			
TEMP2	0.463	-0.818	0.138	0.982	0.152	1.000		
SR	0.130	-0.334	-0.389	0.510	-0.377	0.419	1.000	
DI	0.371	-0.602	0.692	0.451	0.703	0.449	-0.024	1.000

Appendix I. Correlation Matrix of Weather Data

A	B	C	RH	WS (mph)	TEMP (deg C)	A*RH	B*RH	C*RH	A*WS	B*WS	C*WS	A*TEMP	B*TEMP	C*TEMP	RH*WS	RH*TEMP	WS*TEMP	STABIL RATIO	DRIFT INDEX
1	0	0	0.48	4.747	25.86	0.48	0.00	0.00	4.747	0.000	0.000	25.86	0.00	0.00	2.28	12.41	122.75	5.96	14.96
1	0	0	0.58	1.000	24.79	0.58	0.00	0.00	1.000	0.000	0.000	24.79	0.00	0.00	0.58	14.38	24.79	44.40	4.02
1	0	0	0.42	3.224	24.11	0.42	0.00	0.00	3.224	0.000	0.000	24.11	0.00	0.00	1.35	10.12	77.71	8.66	4.95
1	0	0	0.60	2.139	18.80	0.60	0.00	0.00	2.139	0.000	0.000	18.80	0.00	0.00	1.28	11.28	40.23	-1.16	6.06
1	0	0	0.63	1.000	18.33	0.63	0.00	0.00	1.000	0.000	0.000	18.33	0.00	0.00	0.63	11.55	18.33	8.46	11.45
1	0	0	0.45	9.316	20.55	0.45	0.00	0.00	9.316	0.000	0.000	20.55	0.00	0.00	4.19	9.25	191.45	0.48	25.40
1	0	0	0.44	8.032	21.22	0.44	0.00	0.00	8.032	0.000	0.000	21.22	0.00	0.00	3.53	9.34	170.46	0.67	15.91
1	0	0	0.62	7.120	18.70	0.62	0.00	0.00	7.120	0.000	0.000	18.70	0.00	0.00	4.41	11.59	133.14	1.59	13.07
1	0	0	0.44	7.118	20.88	0.44	0.00	0.00	7.118	0.000	0.000	20.88	0.00	0.00	3.13	9.19	148.65	0.84	16.90
1	0	0	0.38	8.400	22.52	0.38	0.00	0.00	8.400	0.000	0.000	22.52	0.00	0.00	3.19	8.56	189.20	0.39	16.87
0	1	0	0.50	4.157	24.97	0.00	0.50	0.00	0.000	4.157	0.000	0.00	24.97	0.00	2.08	12.49	103.79	-0.13	5.31
0	1	0	0.45	1.760	27.34	0.00	0.45	0.00	0.000	1.760	0.000	0.00	27.34	0.00	0.79	12.30	48.12	4.31	5.20
0	1	0	0.80	1.164	15.49	0.00	0.80	0.00	0.000	1.164	0.000	0.00	15.49	0.00	0.93	12.40	18.03	-7.81	3.67
0	1	0	0.66	3.062	22.05	0.00	0.66	0.00	0.000	3.062	0.000	0.00	22.05	0.00	2.02	14.55	67.51	1.39	4.30
0	1	0	0.50	5.427	21.08	0.00	0.50	0.00	0.000	5.427	0.000	0.00	21.08	0.00	2.71	10.54	114.38	0.26	5.19
0	1	0	0.61	3.463	20.50	0.00	0.61	0.00	0.000	3.463	0.000	0.00	20.50	0.00	2.11	12.50	70.98	-3.01	5.47
0	1	0	0.45	3.844	26.54	0.00	0.45	0.00	0.000	3.844	0.000	0.00	26.54	0.00	1.73	11.94	102.02	-2.31	6.13
0	1	0	0.80	6.387	18.28	0.00	0.80	0.00	0.000	6.387	0.000	0.00	18.28	0.00	5.11	14.62	116.75	-0.12	4.15
0	1	0	0.66	7.589	20.29	0.00	0.66	0.00	0.000	7.589	0.000	0.00	20.29	0.00	5.01	13.39	153.95	0.24	4.55
0	1	0	0.56	7.698	22.67	0.00	0.56	0.00	0.000	7.698	0.000	0.00	22.67	0.00	4.31	12.69	174.49	0.04	4.44
0	1	0	0.56	9.076	24.30	0.00	0.56	0.00	0.000	9.076	0.000	0.00	24.30	0.00	5.08	13.61	220.57	-0.24	5.52
0	1	0	0.62	10.105	21.33	0.00	0.62	0.00	0.000	10.105	0.000	0.00	21.33	0.00	6.27	13.23	215.56	0.33	6.58
0	1	0	0.62	8.785	22.08	0.00	0.62	0.00	0.000	8.785	0.000	0.00	22.08	0.00	5.45	13.69	193.97	0.31	5.90
0	1	0	0.71	12.284	18.01	0.00	0.71	0.00	0.000	12.284	0.000	0.00	18.01	0.00	8.72	12.79	221.22	-0.14	6.36
0	1	0	0.63	9.030	18.82	0.00	0.63	0.00	0.000	9.030	0.000	0.00	18.82	0.00	5.69	11.86	169.98	-0.40	6.87
0	0	1	0.78	2.447	15.24	0.00	0.00	0.78	0.000	0.000	2.447	0.00	0.00	15.24	1.91	11.89	37.30	0.54	4.75
0	0	1	0.65	4.502	16.16	0.00	0.00	0.65	0.000	0.000	4.502	0.00	0.00	16.16	2.93	10.50	72.76	0.16	4.80
0	0	1	0.48	3.209	21.35	0.00	0.00	0.48	0.000	0.000	3.209	0.00	0.00	21.35	1.54	10.25	68.50	-0.94	4.77
0	0	1	0.71	5.294	18.61	0.00	0.00	0.71	0.000	0.000	5.294	0.00	0.00	18.61	3.76	13.21	98.52	2.69	4.93
0	0	1	0.55	5.985	20.38	0.00	0.00	0.55	0.000	0.000	5.985	0.00	0.00	20.38	3.29	11.21	121.95	2.00	7.40
0	0	1	0.55	5.478	20.78	0.00	0.00	0.55	0.000	0.000	5.478	0.00	0.00	20.78	3.01	11.43	113.86	-1.08	8.02
0	0	1	0.60	5.420	22.57	0.00	0.00	0.60	0.000	0.000	5.420	0.00	0.00	22.57	3.25	13.54	122.31	-0.20	7.39

Appendix J. Pre-regression Table for StatView

A	B	C	RH	WS (mph)	TEMP (deg C)	A*RH	B*RH	C*RH	A*WS	B*WS	C*WS	A*TEMP	B*TEMP	C*TEMP	RH*WS	RH*TEMP	WS*TEMP	STABIL RATIO	DRIFT INDEX
0	0	1	0.60	4.487	22.33	0.00	0.00	0.60	0.000	0.000	4.487	0.00	0.00	22.33	2.69	13.40	100.19	-1.18	8.73
0	0	1	0.48	6.655	25.02	0.00	0.00	0.48	0.000	0.000	6.655	0.00	0.00	25.02	3.19	12.01	166.52	0.50	6.03
0	0	1	0.46	7.819	25.94	0.00	0.00	0.46	0.000	0.000	7.819	0.00	0.00	25.94	3.61	11.93	203.63	-0.19	6.40
0	0	1	0.55	8.983	21.41	0.00	0.00	0.55	0.000	0.000	8.983	0.00	0.00	21.41	4.94	11.78	192.33	-0.27	6.19
0	0	1	0.68	9.142	17.28	0.00	0.00	0.68	0.000	0.000	9.142	0.00	0.00	17.28	6.22	11.75	157.98	-0.11	5.79
0	0	1	0.50	8.536	25.25	0.00	0.00	0.50	0.000	0.000	8.536	0.00	0.00	25.25	4.27	12.62	215.52	-0.19	5.01
0	0	1	0.38	9.741	22.50	0.00	0.00	0.38	0.000	0.000	9.741	0.00	0.00	22.50	3.70	8.55	219.14	-0.08	11.33
0	0	1	0.38	10.205	22.22	0.00	0.00	0.38	0.000	0.000	10.205	0.00	0.00	22.22	3.88	8.44	226.71	0.04	11.56
0	0	0	0.49	2.237	23.24	0.00	0.00	0.00	0.000	0.000	0.000	0.00	0.00	0.00	1.10	11.39	51.98	1.68	7.07
0	0	0	0.28	1.835	30.47	0.00	0.00	0.00	0.000	0.000	0.000	0.00	0.00	0.00	0.51	8.53	55.91	38.91	8.60
0	0	0	0.33	2.880	31.02	0.00	0.00	0.00	0.000	0.000	0.000	0.00	0.00	0.00	0.95	10.24	89.33	10.50	12.61
0	0	0	0.25	1.520	34.51	0.00	0.00	0.00	0.000	0.000	0.000	0.00	0.00	0.00	0.38	8.63	52.47	60.89	9.59
0	0	0	0.35	1.918	35.74	0.00	0.00	0.00	0.000	0.000	0.000	0.00	0.00	0.00	0.67	12.51	68.54	27.24	14.40
0	0	0	0.32	5.785	30.43	0.00	0.00	0.00	0.000	0.000	0.000	0.00	0.00	0.00	1.85	9.74	176.00	0.98	15.99
0	0	0	0.44	7.496	23.27	0.00	0.00	0.00	0.000	0.000	0.000	0.00	0.00	0.00	3.30	10.24	174.41	1.30	9.89
0	0	0	0.33	6.927	26.71	0.00	0.00	0.00	0.000	0.000	0.000	0.00	0.00	0.00	2.29	8.81	185.01	1.29	17.64
0	0	0	0.62	7.125	18.74	0.00	0.00	0.00	0.000	0.000	0.000	0.00	0.00	0.00	4.42	11.62	133.50	2.23	11.25
0	0	0	0.56	8.406	19.08	0.00	0.00	0.00	0.000	0.000	0.000	0.00	0.00	0.00	4.71	10.68	160.35	0.80	16.80
0	0	0	0.32	13.096	27.97	0.00	0.00	0.00	0.000	0.000	0.000	0.00	0.00	0.00	4.19	8.95	366.24	0.14	41.61
0	0	0	0.32	13.354	29.20	0.00	0.00	0.00	0.000	0.000	0.000	0.00	0.00	0.00	4.27	9.34	389.93	0.17	41.81
0	0	0	0.32	15.695	29.35	0.00	0.00	0.00	0.000	0.000	0.000	0.00	0.00	0.00	5.02	9.39	460.66	0.13	41.50
0	0	0	0.30	16.809	29.23	0.00	0.00	0.00	0.000	0.000	0.000	0.00	0.00	0.00	5.04	8.77	491.37	0.04	41.98
0	0	0	0.29	15.814	29.45	0.00	0.00	0.00	0.000	0.000	0.000	0.00	0.00	0.00	4.59	8.54	465.79	0.03	46.33

Appendix J. (continued)

LEVEL	FACTORS REMOVED	# REMOVED, CUMULATIVE (n)	RSS	RESdf	MSR	F stat	F table	R squared
LEVEL 0	full model	0	273.49	35	7.814	----	----	0.957
LEVEL 1	RH, RH x A,B,C	4	281.28	39	7.212	0.25	2.65	0.956
LEVEL 2	SR, RH x TEMP	6	303.15	41	7.394	0.63	2.38	0.952
LEVEL 3	RH x WS, TEMP x WS	8	329.45	43	7.662	0.90	2.23	0.948
LEVEL 4	A,B,C x TEMP	11	462.50	46	10.054	2.12	2.08	0.928

Appendix K. Multiple Regression Output and Calculations

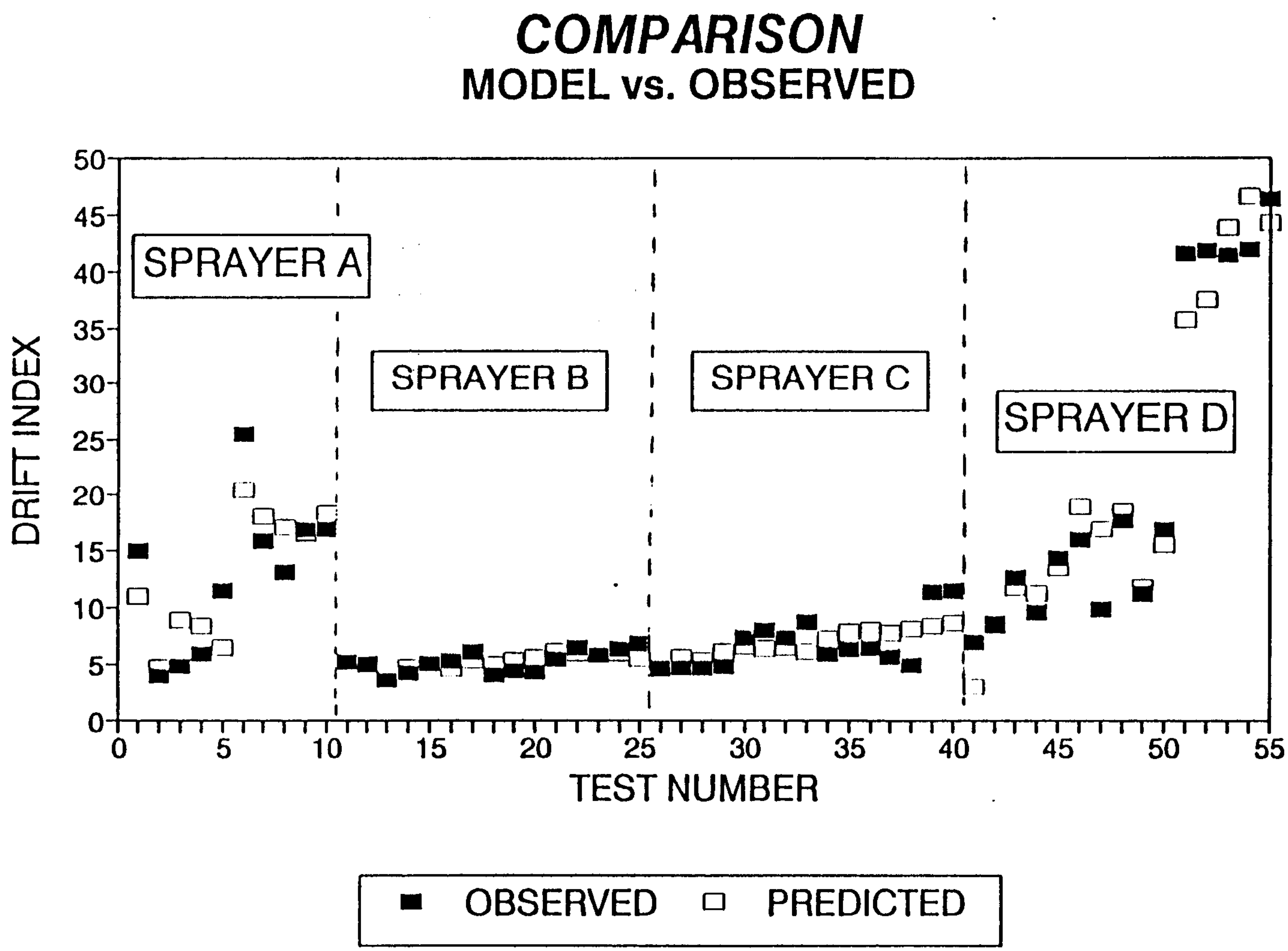

Appendix I.. Comparison of DI Values Using Field Weather Data, Model Prediction vs. Observed

Appendix M. Confidence Intervals for Final Model Coefficients

FACTOR OR INTERACTION	------- 95% --------		------- 90% --------	
	LOWER	UPPER	LOWER	UPPER
A	15.056	51.574	18.095	48.535
B	11.141	40.086	13.550	37.677
C	12.627	39.698	14.880	37.445
D	0.000	0.000	0.000	0.000
WS	1.050	1.292	1.070	1.272
TEMP	0.594	1.203	0.645	1.152
A*WS	-0.686	-0.109	-0.638	-0.157
B*WS	-1.326	-0.846	-1.286	-0.887
C*WS	-1.302	-0.646	-1.248	-0.701
D*WS	0.000	0.000	0.000	0.000
A*TEMP	-1.924	-0.397	-1.797	-0.524
B*TEMP	-1.353	-0.237	-1.260	-0.330
C*TEMP	-1.425	-0.223	-1.325	-0.323
D*TEMP	0.000	0.000	0.000	0.000

Appendix N. Calculation of Drift Index Error

ERROR ANALYSIS CALCULATIONS

Drift Index Formula:

$$DI = \frac{\sum_{i=1}^{10} \{(f_{i+1} + f_i) * (X_{i+1} - X_i)\}}{2 * 1000}$$

where:

DI = drift index
i = downwind station number
(i=1 at 1 m, i=10 at 347 m)
$_i$ = fluorometer reading at station i
X_i = distance downwind from swath at station i (m)

Part 1: Calculating δDI for ± 10 Fluorometer Reading Fluctuation

a. $\delta f_i = \pm 10 = \delta f_R$

b. $\delta f_{i+1} = \pm 10$

c. $\delta(f_i + f_{i+1}) = [(\delta f_i)^2 + (\delta f_{i+1})^2]^{0.5} = 14.14 \equiv K$

d. $\delta\{(f_i + f_{i+1})(X_{i+1} - X_i)\} = dX \bullet \delta(f_i + f_{i+1}) = 14.14\ dX = KdX$

e. $\delta DI = (1/2000) \bullet \{[1K]^2 + [2K]^2 + [4K]^2 + [8K]^2 + [16K]^2 + [32K]^2 + [64K]^2 + [128K]^2 + [91K]^2\}$

$= \pm 1.23$ DI units

Part 2: Calculating δDI for ± 3 String Background Fluorescence

a. $\delta f_i = \pm 3 = \delta f_B$

b. $\delta f_{i+1} = \pm 3$

c. $\delta(f_i + f_{i+1}) = [(\delta f_i)^2 + (\delta f_{i+1})^2]^{0.5} = 4.24 \equiv J$

d. $\delta\{(f_i + f_{i+1})(X_{i+1} - X_i)\} = dX \bullet \delta(f_i + f_{i+1}) = 4.24\ dX = JdX$

e. $\delta DI = (1/2000) \bullet \{[1J]^2 + [2J]^2 + [4J]^2 + [8J]^2 + [16J]^2 + [32J]^2 + [64J]^2 + [128J]^2 + [91J]^2\}$

$= \pm 0.37$ DI units